



**Aerosol
characterization over
the southeastern
United States**

L. Xu et al.

Aerosol characterization over the southeastern United States using high resolution aerosol mass spectrometry: spatial and seasonal variation of aerosol composition, sources, and organic nitrates

L. Xu¹, S. Suresh^{1,*}, H. Guo², R. J. Weber², and N. L. Ng^{1,2}

¹School of Chemical and Biomolecular Engineering, Georgia Institute of Technology, Atlanta, GA, USA

²School of Earth and Atmospheric Sciences, Georgia Institute of Technology, Atlanta, GA, USA

*now at: ExxonMobil, Omaha, NE, USA

Title Page

Abstract

Introduction

Conclusions

References

Tables

Figures



Back

Close

Full Screen / Esc

Printer-friendly Version

Interactive Discussion



Received: 6 March 2015 – Accepted: 18 March 2015 – Published: 9 April 2015

Correspondence to: N. L. Ng (ng@chbe.gatech.edu)

Published by Copernicus Publications on behalf of the European Geosciences Union.

ACPD

15, 10479–10552, 2015

**Aerosol
characterization over
the southeastern
United States**

L. Xu et al.

Title Page

Abstract

Introduction

Conclusions

References

Tables

Figures



Back

Close

Full Screen / Esc

Printer-friendly Version

Interactive Discussion



Abstract

We deployed a High-Resolution Time-of-Flight Aerosol Mass Spectrometer (HR-ToF-AMS) and an Aerosol Chemical Speciation Monitor (ACSM) to characterize the chemical composition of submicron non-refractory particles (NR-PM₁) in the southeastern US. Measurements were performed in both rural and urban sites in the greater Atlanta area, GA and Centreville, AL for approximately one year, as part of Southeastern Center of Air Pollution and Epidemiology study (SCAPE) and Southern Oxidant and Aerosol Study (SOAS). Organic aerosol (OA) accounts for more than half of NR-PM₁ mass concentration regardless of sampling sites and seasons. Positive matrix factorization (PMF) analysis of HR-ToF-AMS measurements identified various OA sources, depending on location and season. Hydrocarbon-like OA (HOA) and cooking OA (COA) have important but not dominant contributions to total OA in urban sites. Biomass burning OA (BBOA) concentration shows a distinct seasonal variation with a larger enhancement in winter than summer. We find a good correlation between BBOA and brown carbon, indicating biomass burning is an important source for brown carbon, although an additional, unidentified brown carbon source is likely present at the rural Yorkville site. Isoprene-derived OA (Isoprene-OA) is only deconvolved in warmer months and contributes 18–36 % of total OA. The presence of Isoprene-OA factor in urban sites is more likely from local production in the presence of NO_x than transport from rural sites. More-oxidized and less-oxidized oxygenated organic aerosol (MO-OOA and LO-OOA, respectively) are dominant fractions (47–79 %) of OA in all sites. MO-OOA correlates well with ozone in summer, but not in winter, indicating MO-OOA sources may vary with seasons. LO-OOA, which reaches a daily maximum at night, correlates better with estimated nitrate functionality from organic nitrates than total nitrates.

Based on the HR-ToF-AMS measurements, we estimate that the nitrate functionality from organic nitrates contributes 63–100 % of total measured nitrates in summer. Further, the contribution of organic nitrates to total OA is estimated to be 5–12 % in summer, suggesting that organic nitrates are important components in the ambient

Aerosol characterization over the southeastern United States

L. Xu et al.

Title Page

Abstract

Introduction

Conclusions

References

Tables

Figures



Back

Close

Full Screen / Esc

Printer-friendly Version

Interactive Discussion



from indirect measurements. For example, Farmer et al. (2010) proposed that the concentration of the nitrate functionality (i.e., $-\text{ONO}_2$) in organic nitrates could be estimated based on the nitrate functionality fragmentation pattern in the AMS or the differences between AMS and ion-chromatography (IC) measurements.

In this study, we performed measurements by a suite of instrumentation in multiple sites in the greater Atlanta area, GA and Centerville, AL, with a focus on a high-resolution time-of-flight aerosol mass spectrometer (HR-ToF-AMS). Positive matrix factorization analysis is performed on HR-ToF-AMS data to identify distinct OA sources. The contribution of organic nitrates to total OA is estimated by different methods based on HR-ToF-AMS measurements. Measurements were performed in both rural and urban sites to investigate the spatial distribution of aerosol in the southeastern US. In addition, measurements spanning over a year allow us to evaluate the seasonal variation of aerosol composition. Our results are not only supported by the available long-term measurements from the SEARCH network, but also provide further insights into interpreting historic measurements.

2 Method

Measurements were conducted at the following sites as part of two field campaigns:

2.1 Southern Oxidant and Aerosol Study (SOAS)

The Southern Oxidant and Aerosol Study (SOAS, <http://soas2013.rutgers.edu/>) is a collaborative field campaign that took place from 1 June to 15 July 2013. The sampling site (32.94°N , 87.18°W) is a SEARCH network site near Centreville in rural Alabama, as shown in Fig. 1. The site is located in a forested area away from large urban cities (55 km SE of Tuscaloosa and 84 km SW of Birmingham, AL). Detailed meteorological conditions of the sampling site can be found in Hidy et al. (2014). In brief, the

Aerosol characterization over the southeastern United States

L. Xu et al.

Title Page

Abstract

Introduction

Conclusions

References

Tables

Figures



Back

Close

Full Screen / Esc

Printer-friendly Version

Interactive Discussion



at each site and repeated it in different seasons. The sampling periods are listed in Table 1.

While the trailer was rotated between multiple sites, we also deployed an Aerosol Chemical Speciation Monitor (ACSM, described in Sect. 2.3.2) (Ng et al., 2011) at the Georgia Tech site from May 2012 to February 2013. The paired and simultaneous measurements using an ACSM at the Georgia Tech site and a High Resolution Time-of-Flight Aerosol Mass Spectrometer (HR-ToF-AMS, described in Sect. 2.3.1) rotating among four different sites allow for the investigation of the spatial distribution of aerosol loading and composition in the greater Atlanta area. It is noted that from 20 July to 4 September 2012, both the HR-ToF-AMS and the ACSM were deployed at the Georgia Tech site for instrument inter-comparison.

2.3 Instrumentation

2.3.1 High Resolution Time-of-Flight Aerosol Mass Spectrometer (HR-ToF-AMS)

An Aerodyne High-Resolution Time-of-Flight Aerosol Mass Spectrometer (HR-ToF-AMS) was rotated among different sites in this study to characterize the composition of ambient submicron non-refractory particulate matter (NR-PM₁). A detailed description of the HR-ToF-AMS can be found in literature (Canagaratna et al., 2007; DeCarlo et al., 2006). In brief, the HR-ToF-AMS focuses ambient particles with vacuum aerodynamic diameter smaller than 1 μm into a narrow beam by using an aerodynamic lens. The submicron particles are then impacted on a hot tungsten surface (~ 600 °C), where non-refractory species are flash evaporated. The resultant vapors are ionized using 70 eV electron impact ionization and analyzed by a time-of-flight mass spectrometer. During sampling, a PM₁ cyclone was used to remove coarse particles. A nafion-dryer was placed upstream of the HR-ToF-AMS to dry the particles (relative humidity < 20 %) in order to eliminate the potential influence of relative humidity on particle collection efficiency (CE) at the vaporizer (Matthew et al., 2008). Gas-phase interference was elimi-

Aerosol characterization over the southeastern United States

L. Xu et al.

Title Page

Abstract

Introduction

Conclusions

References

Tables

Figures



Back

Close

Full Screen / Esc

Printer-friendly Version

Interactive Discussion



1.4, 1.1, and 1.3, respectively. RIE values of 4.18 and 0.59 were used for ammonium and sulfate, which were determined from IE calibrations by using ammonium nitrate and ammonium sulfate particles.

2.3.3 Co-located instruments

5 In addition to the HR-ToF-AMS, we deployed various instruments in the trailer while performing measurements at multiple sites (Verma et al., 2014). Instruments of interest to this study includes a PILS-LWCC-TOC system (Particle Into Liquid Sampler – Liquid Waveguide Capillary Cell – Total Organic Carbon analyzer), which was deployed to measure the light absorption spectra of water-soluble organic components. Detailed working principle of the PILS-LWCC-TOC system can be found in Hecobian et al. (2010). The average light absorption between 360 to 370 nm is used as a measure of brown carbon. Black carbon concentration was measured by either a seven-wavelength Aethalometer or a multi-angle absorption photometer (MAAP). For Aethalometer, the measurements under seven wavelengths (i.e., 370, 450, 571, 590, 15 660, 880, and 950 nm) were averaged to represent the black carbon concentration. The measured data were corrected for loading effects (Virkkula et al., 2007).

At the Jefferson Street site (JST) and Yorkville site (YRK), a suite of instruments was operated by the SEARCH Network. Detailed description about the collocated instruments can be found in Hansen et al. (2003) and Edgerton et al. (2005). In brief, O₃ 20 concentration was measured by a UV-absorption analyzer. NO and NO_x were measured by a chemiluminescence analyzer, where the NO₂ concentration was calculated by subtracting NO from the total NO_x. PM_{2.5} sulfate and OC were continuously measured by a Fe reduction/UV-fluorescence analyzer and an oxidative combustion (R&P 5400) analyzer, respectively. Meteorological conditions, such as temperature, relative 25 humidity (RH), solar radiation, and wind speed were also recorded.

**Aerosol
characterization over
the southeastern
United States**

L. Xu et al.

Title Page

Abstract

Introduction

Conclusions

References

Tables

Figures



Back

Close

Full Screen / Esc

Printer-friendly Version

Interactive Discussion



2.4 Positive Matrix Factorization (PMF) analysis

Positive Matrix Factorization (PMF) is a mathematical technique to solve bilinear unmixing problems (Paatero, 1997; Paatero and Tapper, 1994). PMF analysis has been widely applied in the aerosol community for source apportionment (Ulbrich et al., 2009; Jimenez et al., 2009; Zhang et al., 2010; Lanz et al., 2007; Ng et al., 2010). For the data measured by AMS, PMF analysis represents the observed data matrix as a linear combination of various factors with constant mass spectrum but varying concentrations across the dataset (Ulbrich et al., 2009; Zhang et al., 2011). To determine the sources of organic aerosol, PMF analysis was performed on the high-resolution organic mass spectra (m/z 12–200) obtained by the HR-ToF-AMS for each sampling dataset. We generated the organic data matrix and error matrix from PIKA v1.12 and pretreated the error matrix by using PMF Evaluation Toolkit (PET) software and following the procedure described in Ulbrich et al. (2009). m/z 's with signal-to-noise smaller than 0.2 are removed and m/z 's with signal-to-noise ranging between 0.2 and 2 are downweighted by a factor of 2. We downweighted the errors of O^+ , HO^+ , H_2O^+ , and CO^+ , which are related to CO_2^+ organic ions, to avoid excessive weighting of CO_2^+ . In addition, for four datasets (JST_May, CTR_June, YRK_July, and GT_August), the error of CHO^+ is downweighted by a factor of 4 because PIKA v1.12 appears to underestimate CHO^+ error, which is possibly caused by that the overlap of the CHO^+ (m/z 29.0027) ion with its adjacent N_2 isotope ion ($j15NN$, m/z 29.0032). For the other three datasets (JST_Nov, YRK_Dec, and RS_Jan), CHO^+ is not included in the PMF analysis due to its occasionally negative signals, which is likely caused by a low CHO^+ signal in winter. At times, the CHO^+ concentration is near the detection limit, so that a shift in threshold might cause the CHO^+ signal to be treated as noise. PMF solutions were carefully evaluated according to the procedure outlined in Zhang et al. (2011). For each dataset, the optimal solution was determined after examining the residuals of PMF fits, interpretability of factor's diurnal trend, factor correlation with external tracers, and characteristic signature in factor mass spectrum. The rotational ambiguity of solutions were

Title Page

Abstract

Introduction

Conclusions

References

Tables

Figures



Back

Close

Full Screen / Esc

Printer-friendly Version

Interactive Discussion



examined by changing the parameter FPEAK and the robustness of solutions were evaluated by starting PMF with different initial conditions (parameter SEED). The key diagnostic plots for all datasets are shown in Fig. S1. An FPEAK value of 0 is used for all datasets in our analysis, because the use of FPEAK values that are different from 0 do not improve the correlations between PMF factors with external tracers.

2.5 Estimation of organic nitrates contribution to ambient OA

As direct measurements of organic nitrates are not available, we estimate the concentration of particle-phase organic nitrates at each site based on HR-ToF-AMS measurements in this study. It is important to note that total nitrates measured by the HR-ToF-AMS (denoted as $\text{NO}_{3,\text{meas}}$) is the nitrate functionality ($-\text{ONO}_2$) which could arise from both inorganic and organic nitrates. Here, we apply two independent methods in separating the measured total nitrates into nitrate functionality from inorganic and organic nitrates. In the following discussion, we use the subscripts $_{\text{meas}}$, $_{\text{inorg}}$, and $_{\text{org}}$ to denote nitrate functionality ($-\text{ONO}_2$) or fragments (NO^+ and NO_2^+) from total nitrates (measured), inorganic nitrates (calculated), and organic nitrates (calculated), respectively.

The first method is based on the $\text{NO}^+/\text{NO}_2^+$ ratio (denoted as NO_x^+ ratio method for discussions hereafter) in the AMS mass spectra (Farmer et al., 2010). Due to the extensive fragmentation caused by 70 eV electron ionization in the HR-ToF-AMS, the nitrate functionality ($-\text{ONO}_2$) fragments to produce NO^+ and NO_2^+ ions. Previous laboratory studies have shown that the $\text{NO}^+/\text{NO}_2^+$ ratio in the aerosol mass spectrum is substantially higher for organic nitrates than ammonium nitrate (AN) (Bruns et al., 2010; Fry et al., 2009; Sato et al., 2010; Farmer et al., 2010; Boyd et al., 2015), which is the major source of PM_1 inorganic nitrates in the southeast US that can be detected by AMS (Guo et al., 2014; Allan et al., 2004). For example, while the $\text{NO}^+/\text{NO}_2^+$ ratio is about 2.4 for ammonium nitrate, the ratio ranges from 5 to 10 for SOA derived from isoprene + NO_3^\bullet and β -pinene + NO_3^\bullet reactions, respectively (Bruns et al., 2010; Boyd et al., 2015). In addition to organic nitrates produced from biogenic VOC oxidation, Sato et al. (2010) showed that the NO_x^+ ratio of organic nitrates from the photooxidation of aromatic hy-

Aerosol characterization over the southeastern United States

L. Xu et al.

Title Page

Abstract

Introduction

Conclusions

References

Tables

Figures

◀

▶

◀

▶

Back

Close

Full Screen / Esc

Printer-friendly Version

Interactive Discussion



drocarbons is also clearly higher than that of ammonium nitrate (3.8–5.8 vs. 1.1–2.8). Based on the differences in NO_x^+ ratio between organic and inorganic nitrates, Farmer et al. (2010) proposed that the concentrations of NO_{org} and $\text{NO}_{2,\text{org}}$ can be estimated from NO_{meas} and $\text{NO}_{2,\text{meas}}$ by Eqs. (1) and (2).

$$\text{NO}_{2,\text{org}} = \frac{\text{NO}_{2,\text{meas}} \times (R_{\text{meas}} - R_{\text{AN}})}{R_{\text{ON}} - R_{\text{AN}}} \quad (1)$$

$$\text{NO}_{\text{org}} = R_{\text{ON}} \times \text{NO}_{2,\text{org}} \quad (2)$$

R_{meas} is the NO_x^+ ratio from observation. R_{AN} is the NO_x^+ ratio for pure ammonium nitrate (AN), which has been reported to depend on instrument performance and vary between different instruments (Farmer et al., 2010; Rollins et al., 2010). In this study, we determine the R_{AN} of each dataset from Ionization Efficiency (IE) calibrations using 300 nm ammonium nitrate particles. We find that R_{AN} varies between 1.73 and 2.93 (Table 2), which is within the range (1.1–3.5) reported in literature (Sato et al., 2010; Farmer et al., 2010; Sun et al., 2012b; Fry et al., 2013). R_{ON} is the NO_x^+ ratio for organic nitrates. Similar to R_{AN} , R_{ON} also varies between instruments (Boyd et al., 2015; Bruns et al., 2010; Fry et al., 2009). Thus, the R_{ON} values reported in the literature cannot be directly applied in our datasets. In order to circumvent this issue, Fry et al. (2013) assumed that the $R_{\text{ON}}/R_{\text{AN}}$ value is instrument independent. The authors further obtained R_{ON} by multiplying R_{AN} determined from in-field IE calibrations with $R_{\text{ON}}/R_{\text{AN}}$ determined from six organic nitrate standards (average value = 2.25). However, the reported $R_{\text{ON}}/R_{\text{AN}}$ values in the literature vary for different organic nitrates. For example, while the average $R_{\text{ON}}/R_{\text{AN}}$ value is 2.25 for the organic nitrate standards in Farmer et al. (2010), the $R_{\text{ON}}/R_{\text{AN}}$ ranges from 3.70 to 4.17 for organic nitrates produced from β -pinene oxidation by nitrate radicals (Boyd et al., 2015; Bruns et al., 2010; Fry et al., 2009). Considering the large variations in $R_{\text{ON}}/R_{\text{AN}}$ values and unknown contributions from different organic nitrates, we apply the NO_x^+ ratio method to obtain an estimation range by using extreme R_{ON} values. We select organic nitrates formed from isoprene and monoterpene oxidations as representative because of their large abundance in

Aerosol characterization over the southeastern United States

L. Xu et al.

Title Page

Abstract

Introduction

Conclusions

References

Tables

Figures

◀

▶

◀

▶

Back

Close

Full Screen / Esc

Printer-friendly Version

Interactive Discussion



**Aerosol
characterization over
the southeastern
United States**

L. Xu et al.

Title Page

Abstract

Introduction

Conclusions

References

Tables

Figures



Back

Close

Full Screen / Esc

Printer-friendly Version

Interactive Discussion



the southeastern US, potential to produce organic nitrates, and that they cover a wide range of $R_{\text{ON}}/R_{\text{AN}}$ values (i.e., 2.08 for isoprene and 3.70–4.17 for β -pinene) (Boyd et al., 2015; Bruns et al., 2010; Fry et al., 2009). Though the photooxidation of aromatic VOCs could also produce organic nitrates, their $R_{\text{ON}}/R_{\text{AN}}$ ratio is close to that of isoprene organic nitrates (Sato et al., 2010). Multiplying the average R_{AN} (i.e., 2.28 ± 0.40) of all datasets in this study by the average $R_{\text{ON}}/R_{\text{AN}}$ ratio of isoprene (i.e., 2.08) and β -pinene organic nitrates (i.e., 3.99 ± 0.25) in the literature (Boyd et al., 2015; Bruns et al., 2010; Fry et al., 2009), within one SD we selected 5 (i.e., 4.74 ± 0.83) and 10 (i.e., 9.10 ± 1.69) as the lower and upper values of R_{ON} . It is important to note that R_{ON} values of 5 and 10 likely correspond to upper and lower bounds of the $\text{NO}_{3,\text{org}}$ concentrations estimated by the NO_x^+ ratio method. The assumption that $R_{\text{ON}}/R_{\text{AN}}$ is instrument independent warrants further study.

The second method is based on PMF analysis (denoted as PMF method). In addition to PMF analysis on organic mass spectra (denoted as PMF_{org}), we have also performed PMF analysis on organic mass spectra together with NO^+ and NO_2^+ ions (denoted as $\text{PMF}_{\text{org}+\text{NO}_3}$). Such analysis could provide useful insights regarding the relative contributions of organic and inorganic nitrates. For instance, Sun et al. (2012b) and Hao et al. (2014) performed PMF analysis on merged mass spectra with both organic and inorganic signals from HR-ToF-AMS measurements. The authors showed that the NO^+ and NO_2^+ fragments are distributed among a nitrate inorganic aerosol (NIA) factor and other organic aerosol factors.

In this study, the selection of optimal solutions for PMF analysis on the merged mass spectra (i.e. $\text{PMF}_{\text{org}+\text{NO}_3}$) is discussed in detail in the Supplement. In brief, in addition to examining the typical diagnostic plots (Fig. S3), the optimal solutions are selected by comparing the time series (Fig. S5), mass spectrum (Fig. S5), and mass concentration (Fig. S6) with results from PMF_{org} . After determining the optimal solution of $\text{PMF}_{\text{org}+\text{NO}_3}$, the concentrations of “nitrate functionality from organic nitrates” (i.e., $\text{NO}_{3,\text{org}}$) are calculated by summing up the nitrate signals (i.e., NO^+ and NO_2^+) from all

OA factors by the following equations.

$$[\text{NO}_{\text{org}}^+] = \sum ([\text{OA factor}]_i \times f_{\text{NO}_i}) \quad (3)$$

$$[\text{NO}_{2,\text{org}}^+] = \sum ([\text{OA factor}]_i \times f_{\text{NO}_{2,i}}) \quad (4)$$

where $[\text{OA factor}]_i$ is the mass concentration of the i th OA factor, f_{NO_i} and $f_{\text{NO}_{2,i}}$ are the mass fraction of NO^+ and NO_2^+ , respectively, in i th OA factor. For both the NO_x^+ ratio method and PMF method, we calculate the concentration of $\text{NO}_{3,\text{inorg}}$ (i.e., nitrate functionality from inorganic nitrates) by subtracting $\text{NO}_{3,\text{org}}$ (i.e., nitrate functionality from organic nitrates) from $\text{NO}_{3,\text{meas}}$ (i.e., total measured nitrates).

3 Results

Table 1 lists the meteorology parameters (temperature, relative humidity, and wind speed), gas-phase concentrations of NO , NO_2 , and O_3 , and aerosol compositions of the seven datasets reported in this study. The average RH is above 60% for all the datasets with little seasonal variation, which is consistent with previous observations (Ford and Heald, 2013). The high RH in the southeastern US has direct impacts on particle water content and particle acidity. Recently, Guo et al. (2014) showed that particle water and acidity are mainly driven by the variability of RH, although particle composition also plays a role. The average wind speed is relatively constant ($1.3\text{--}3.4 \text{ m s}^{-1}$) throughout the year at all sites. NO_x (NO and NO_2) and black carbon (BC), which are tracers for anthropogenic emissions, are lower in the rural Yorkville (YRK) site than the urban Jefferson Street (JST) site. In YRK, NO_x level is low (i.e., average concentration $< 0.3 \text{ ppb}$) in all seasons. In contrast, at the urban JST site, NO_x level is elevated in winter compared to summer, indicating more anthropogenic emissions in winter at urban sites.

Figure 2 shows the composition of non-refractory submicron particulate matter (NR- PM_1) of all datasets. Organics are the dominant components, which account for more

which have large emissions of POA and BC, gasoline vehicles have a larger emission of VOCs (e.g., toluene and benzene) (Platt et al., 2013). Secondly, in addition to vehicle type, the evaporation of POA emitted from vehicles would further decrease its mass concentration. Robinson et al. (2007) showed that POA from vehicle emission is indeed semi-volatile, which would evaporate substantially upon dilution from tailpipe to ambient conditions (a dilution ratio of 10^3 to 10^4). Thirdly, HOA tends to contribute a small fraction of OA because of the high level of regional background OA in the greater Atlanta area. For example, OOA factors (i.e., LO-OOA and MO-OOA) compromise 47–79 % of OA as shown in Fig. 5. The effect of wind direction on HOA concentration is expected to be small considering the close proximity of the roadside sampling site to the highway.

4.1.2 COA

The mass spectrum of cooking organic aerosol (COA) is characterized by prominent signal at ion $C_3H_5^+$ (m/z 41) and $C_4H_7^+$ (m/z 55) (Fig. S2), which could arise from the heating of seed oil (Allan et al., 2010). Another feature of COA is its clear and unique diurnal trend, which exhibits a small peak at lunch time and a large peak at dinner time (Fig. 6). The COA factor is identified in urban sites (JST site, GT site, and RS site) throughout the year, with the mass fraction varying from 12–20 %. A prior study by Zheng et al. (2002) estimated that meat cooking accounts for 5–12 % of $PM_{2.5}$ organic carbon in the southeastern US by using chemical mass balance receptor model. The range reported by Zheng et al. (2002) is similar to our study, considering the differences in sampling periods, particle size range, and estimation method. The COA factor has also been detected in many megacities around the world (Huang et al., 2010; Allan et al., 2010; Slowik et al., 2010; Mohr et al., 2012; Crippa et al., 2013), indicating cooking is an important OA source in megacities.

We note that the COA factor was not resolved in Budisulistiorini et al. (2013), in which the authors performed PMF analysis on the data collected by an Aerosol Chemical Speciation Monitor (ACSM) at the JST site in 2011 summer and fall. The lack of a COA factor in the analysis by Budisulistiorini et al. (2013) could be a result of the lower

resolution (unit mass resolution) of the ACSM compared to HR-ToF-AMS (Ng et al., 2011). Previous studies have suggested that COA is not easily differentiated from HOA due to the similarity of their mass spectra in unit mass resolution data (Crippa et al., 2014; Mohr et al., 2009).

4.1.3 Isoprene-OA

The Isoprene-OA factor is characterized by prominent signals at ion $C_4H_5^+$ (m/z 53) and $C_5H_6O^+$ (m/z 82) in its mass spectrum (Fig. S2), which resembles that of isoprene SOA formed via IEPOX uptake in the presence of hydrated sulfate in laboratory experiments (Lin et al., 2012; Budisulistiorini et al., 2013; Nguyen et al., 2014; Liu et al., 2014). For our datasets, Isoprene-OA is only identified in warmer months (May–August) and accounts for 18–36 % of total OA (Fig. 5). The seasonal variation of Isoprene-OA factor is consistent with that of isoprene emissions, which are high in summer and nearly zero in winter (Guenther et al., 2006). The identification of the Isoprene-OA factor could be further supported by its correlation with methyltetrols, which are products formed from isoprene oxidation and likely via IEPOX uptake. For the Centreville dataset where methyltetrols were continuously measured by a semi-volatile thermal desorption aerosol gas chromatograph (SV-TAG) (Isaacman et al., 2014), the correlation (Pearson's R) between the Isoprene-OA factor and methyltetrols is found to be 0.68 (Xu et al., 2015).

The ratio of $C_5H_6O^+$ to total signal of isoprene-OA factor, $f_{C_5H_6O^+}$, which is used as a characteristic marker for SOA formed via IEPOX uptake in the literature, ranges from 0.9–2.3 % in this study. This range is similar to the values from other ambient data (Budisulistiorini et al., 2013; Chen et al., 2014; Robinson et al., 2011a; Slowik et al., 2011), but lower than that from laboratory-generated fresh SOA from IEPOX uptake (3.6 % from Liu et al., 2014). We note that the $f_{C_5H_6O^+}$ is higher at rural sites (1.9 % for YRK_July and 2.3 % for CTR_June) than urban sites (0.9 % for JST_May and 1.4 % for GT_August). Similarly, Liu et al. (2014) observed that the mass spectrum of laboratory-generated SOA from IEPOX uptake has a stronger correlation with that

**Aerosol
characterization over
the southeastern
United States**

L. Xu et al.

Title Page

Abstract

Introduction

Conclusions

References

Tables

Figures

◀

▶

◀

▶

Back

Close

Full Screen / Esc

Printer-friendly Version

Interactive Discussion



by PMF analysis in this study, the correlation between BBOA and brown carbon is greater than 0.69, with the best correlation observed at JST_Nov ($R = 0.90$) (Fig. 7). The correlation between BBOA and brown carbon is only 0.47 for YRK_Dec, which is likely caused by other brown carbon sources at the YRK site. This hypothesis could be supported by the summer measurements in YRK. In YRK_July, we observed a large abundance of brown carbon, which reaches daily maximum around 2 p.m. (Fig. S8); however, a BBOA factor is not resolved for YRK_July, indicating that brown carbon, in this case, could arise from sources other than biomass burning. Hecobian et al. (2010) suggested that SOA from aqueous phase reactions may be an important source for brown carbon in summer based on analysis on ~ 900 filters collected in 2007 in the southeastern US. A recent laboratory study showed that SOA from IEPOX reactive uptake could be light-absorbing and potentially an important source for brown carbon (Lin et al., 2014). However, Isoprene-OA factor, which is related to the IEPOX uptake pathway studied in Lin et al. (2014), only shows weak correlation (R ranges from 0.22 to 0.50) with brown carbon as shown in Fig. S9. As suggested by Washenfelder et al. (2015), the difference between ambient observation and laboratory studies might be due to that the IEPOX-derived absorbing chromophores do not dominate the Isoprene-OA mass. However, further studies are warranted to resolve this difference.

4.1.5 MO-OOA

Two oxygenated OA factors (MO-OOA and LO-OOA) with high, but differing O : C ratios, were identified in both rural and urban sites throughout the year. Based on their inferred volatility from O : C ratios, OOA factors are typically named as low-volatility OOA (higher O : C and lower volatility) and semi-volatile OOA (lower O : C and higher volatility) (Ng et al., 2010; Jimenez et al., 2009). However, recent studies showed that O : C ratios are not always well-correlated with aerosol volatility (Hildebrandt et al., 2010; Xu et al., 2014). Thus, in this study, we use the terms “more-oxidized OOA” (MO-OOA, O : C ranges between 0.66 and 1.05, with an average of 0.87) and “less-oxidized OOA” (LO-OOA, O : C ranges between 0.44 and 0.62, with an average of 0.54) (Fig. S10). This

radiocarbon analysis. For example, if the majority of MO-OOA in winter has non-fossil sources, it could suggest that aged OA from biomass burning is an important source for MO-OOA, because biomass burning is enhanced and the emissions of biogenic VOCs are low in winter.

4.1.6 LO-OOA

Similar to MO-OOA, less-oxidized oxygenated organic aerosol (LO-OOA) is also observed in both rural and urban sites throughout the year. LO-OOA comprises 19–34 % of total OA (Fig. 5). A key feature of LO-OOA is that it consistently exhibits a daily maximum at early morning and night in all datasets (Fig. 6). The similar diurnal variation of LO-OOA has also been observed in previous field measurements and thought to be primarily driven by the semi-volatile nature of LO-OOA. The LO-OOA factor identified in multiple prior field measurements has been observed to correlate with ammonium nitrate, a semi-volatile species which mainly partitions into the particle phase at night when the temperature is relatively low (Jimenez et al., 2009; Sun et al., 2012a; Zhang et al., 2011; Ulbrich et al., 2009). However, in this study, LO-OOA only shows moderate correlation with total NO_3 (i.e., $\text{NO}_{3,\text{meas}}$) measured by the HR-ToF-AMS in summer datasets (R ranges between 0.56 and 0.76) and no correlation in winter datasets (R ranges between 0.14 and 0.46) (Fig. 9 and Table 2).

While LO-OOA only moderately or sometimes poorly correlates with $\text{NO}_{3,\text{meas}}$ in this study, we find improved correlation between LO-OOA and “nitrate functionality from organic nitrates” (i.e., $\text{NO}_{3,\text{org}}$) (Fig. 9 and Table 2). $\text{NO}_{3,\text{org}}$ is estimated by using NO_x^+ ratio method as described in Sect. 2.5. A R_{ON} value of 10 is applied since different R_{ON} values would only affect the estimated concentration of $\text{NO}_{3,\text{org}}$, but not the correlation between LO-OOA and $\text{NO}_{3,\text{org}}$, because estimated $\text{NO}_{3,\text{org}}$ has a linear relationship with R_{ON} . For most datasets, LO-OOA correlates better with $\text{NO}_{3,\text{org}}$ than total nitrates. The biggest improvement is seen in JST_Nov, where the correlation R increases from 0.14 to 0.63. However, we also note that the correlation becomes worse for YRK_Dec and RS_Jan, which is likely caused by the small contribution of organic nitrates to total

Aerosol
characterization over
the southeastern
United States

L. Xu et al.

Title Page

Abstract

Introduction

Conclusions

References

Tables

Figures



Back

Close

Full Screen / Esc

Printer-friendly Version

Interactive Discussion



in JST_May and GT_August) than colder months (16–38% in JST_Nov, YRK_Dec, and RS_Jan) (Fig. S11). The fact that the $\text{NO}^+/\text{NO}_2^+$ ratio of the NIA factor resolved from warmer months is higher than that of pure ammonium nitrate (Fig. S12) is also indicative of organic nitrate interference in the NIA factor. Conversely, the $\text{NO}^+/\text{NO}_2^+$ ratio of the NIA factor resolved from colder months is closer to that of pure ammonium nitrate, suggesting less interference from organics. Thus, for the sites where a NIA factor is identified, the presence of organic nitrates in the NIA factor would result in an underestimation of $\text{NO}_{3,\text{org}}$, and the underestimation is larger for warmer months (i.e., JST_May and GT_August). For CTR_June and YRK_July, the NIA factor is not resolved from PMF_{org+NO₃} analysis, likely due to a small concentration of inorganic nitrates. For example, the concentrations of organics and total nitrates (i.e., $\text{NO}_{3,\text{meas}}$) are 5.0 and 0.1 $\mu\text{g m}^{-3}$, respectively, for CTR_June. Even if one assumes that all the measured nitrates arise from inorganic nitrates, the nitrates / organics ratios is only 2%, making it difficult for PMF to retrieve the NIA factor accurately (Ulbrich et al., 2009). Thus, for CTR_June and YRK_July, the small amount of $\text{NO}_{3,\text{inorg}}$, which is not retrievable by PMF, was attributed into OA factors so that the PMF method would slightly overestimate $\text{NO}_{3,\text{org}}$.

For the NO_x^+ ratio method, considering the large variation in NO_x^+ ratio for different organic nitrates, the largest uncertainty is associated with the value of R_{ON} . Ideally, the time-dependent R_{ON} values should be applied. However, this is challenging because the determination of time-dependent R_{ON} requires measurements of every ambient organic nitrate species, which are not available. With this, we apply R_{ON} values of 5 and 10 in our analysis to provide the upper and lower bounds of the estimated $\text{NO}_{3,\text{org}}$ concentration for the NO_x^+ ratio method as discussed in Sect. 2.5. It is noted that for Centreville, we applied a third method to calculate the concentration of $\text{NO}_{3,\text{org}}$, which is based on the differences between HR-ToF-AMS measurements (NO_3 from both organic and inorganic species) and PILS-IC measurements (NO_3 from inorganic species only) (Xu et al., 2015; Bae et al., 2007; Orsini et al., 2003). This method, denoted as AMS-IC method, is only applied for Centreville because PILS-IC was not deployed

Aerosol characterization over the southeastern United States

L. Xu et al.

Title Page

Abstract

Introduction

Conclusions

References

Tables

Figures



Back

Close

Full Screen / Esc

Printer-friendly Version

Interactive Discussion



**Aerosol
characterization over
the southeastern
United States**

L. Xu et al.

Title Page

Abstract

Introduction

Conclusions

References

Tables

Figures

◀

▶

◀

▶

Back

Close

Full Screen / Esc

Printer-friendly Version

Interactive Discussion



in the SCAPE study. In order to match the HR-ToF-AMS particle cut size (i.e., PM_{10}), a PM_{10} cyclone was deployed at the inlet of PILS-IC. However, due to the transmission efficiency of PM_{10} cyclone, PILS-IC measurements might have interferences from particles larger than $1\ \mu\text{m}$ (i.e., NaNO_3 in mineral dust). The interferences are expected to be small because the sodium concentration measured by PILS-IC with PM_{10} cyclone is negligible and mostly below its detection limit ($0.07\ \mu\text{g m}^{-3}$) (Fig. S13). As shown in Fig. 11, The $\text{NO}_{3,\text{org}}$ estimated by the AMS-IC method falls within the range of NO_x^+ ratio method, which is defined by R_{ON} values of 5 and 10, indicating the feasibility to use these two values as the upper and lower bounds to estimate $\text{NO}_{3,\text{org}}$ for the NO_x^+ ratio method.

Based on the uncertainties of the PMF method and the NO_x^+ ratio method, we could explain the differences between the two methods and further combine them in order to narrow the estimation range. According to the extent of agreement between the two methods, all seven datasets are grouped into three categories: summer months (CTR_June and YRK_July), transition months (JST_May and GT_August), and winter months (JST_Nov, YRK_Dec, and RS_Jan).

For winter months, the PMF method shows good agreement with the NO_x^+ ratio method with a R_{ON} value of 10 for JST_Nov and YRK_Dec. This is consistent with the observations that the interference of organic nitrates in the NIA factor is small in winter datasets (Figs. S11 and S12) and isoprene emission is negligible in winter (Guenther et al., 2006). Thus, results from the NO_x^+ ratio method with $R_{\text{ON}} = 5$ (i.e., isoprene organic nitrates) are likely unrealistic. With this, we combine the results from the PMF method and the NO_x^+ ratio method with $R_{\text{ON}} = 10$ as the “best estimate” range of organic nitrates for JST_Nov and YRK_Dec. For RS_Jan, the NO_x^+ ratio method predicts negative $\text{NO}_{3,\text{org}}$ due to R_{meas} being smaller than R_{AN} at times (Eq. 1). In this case, the PMF method is selected as the “best estimate”. Taken together, the mass fraction of organic nitrates (i.e., $\text{NO}_{3,\text{org}}/\text{NO}_{3,\text{meas}}$) is 0.19–0.21, 0.11–0.21, and ~ 0.10 for JST_Nov, YRK_Dec, and RS_Jan, respectively.

**Aerosol
characterization over
the southeastern
United States**

L. Xu et al.

Title Page

Abstract

Introduction

Conclusions

References

Tables

Figures

◀

▶

◀

▶

Back

Close

Full Screen / Esc

Printer-friendly Version

Interactive Discussion

For summer months, the PMF method predicts that all the measured nitrates are from organic nitrates are (i.e., $\text{NO}_{3,\text{org}}/\text{NO}_{3,\text{meas}} = 1$, Fig. 10), because a NIA factor is not resolved from PMF analysis and that all the measured NO_3 are distributed in the OA factors. The $\text{NO}_{3,\text{org}}$ estimated from the PMF method falls within the upper (i.e., $R_{\text{ON}} = 5$) and lower bound (i.e., $R_{\text{ON}} = 10$) of the NO_x^+ ratio method (Fig. 10). For CTR_June, the NO_x^+ ratio method with R_{ON} value of 5 predicts a $\text{NO}_{3,\text{org}}/\text{NO}_{3,\text{meas}}$ ratio that is greater than 1, which results from the assumed R_{ON} value (i.e., 5) being smaller than R_{meas} at times (Eq. 1). Thus, the PMF method and the NO_x^+ ratio method with $R_{\text{ON}} = 10$ define the upper and lower bound, respectively. Accordingly, the “best estimate” range of $\text{NO}_{3,\text{org}}/\text{NO}_{3,\text{meas}}$ is 0.80–1 and 0.63–1 for CTR_June and YRK_July, respectively.

For transition months (i.e., JST_May and GT_Aug, the sampling periods of which were between summer and winter), the PMF method and the NO_x^+ ratio method show large discrepancies. Compared to PMF method, the NO_x^+ ratio method predicts 1.5–2.5 times higher $\text{NO}_{3,\text{org}}$ concentration depending on site and R_{ON} value. This is likely caused by the PMF method under-predicting $\text{NO}_{3,\text{org}}$ owing to the attribution of some organic nitrates to the NIA factor. Thus, we select the NO_x^+ ratio method with R_{ON} values of 5 and 10 as the “best estimate” range. Accordingly, $\text{NO}_{3,\text{org}}/\text{NO}_{3,\text{meas}}$ ranges 0.55–0.76 and 0.64–0.99 for JST_May and GT_Aug, respectively.

Further, we calculate the contribution of organic nitrate molecules to OA from “best-estimate” range of nitrate functionality (i.e., $\text{NO}_{3,\text{org}}$). We assume that particle-phase organic nitrates have an average molecule weight of 200 and 300 g mol^{-1} (Rollins et al., 2012), which provides an lower and upper bound for estimated concentration of organic nitrates. As shown in Fig. 10, organic nitrates contribute about 5–12 % of total OA for summer datasets (CTR_June and YRK_July) and 9–25 % of total OA for winter datasets (JST_Nov, YRK_Dec, and RS_Jan), suggesting that organic nitrates are important components of total OA in the southeastern US.

5 Conclusions

Nearly one-year measurements were performed across multiple sites in the southeastern US with a variety of online instruments, with the focus on HR-ToF-AMS data in this study. We find that organics are the dominant components of the NR-PM₁ at both rural and urban sites throughout the year. The OA diurnal profile shows little variation in summer and peaks at night in winter datasets. The lack of midday enhancement in OA diurnal profile is likely caused by the expansion of boundary layer in the day and compensating effects of various OA factors. The OA measured at different sampling sites and seasons has a similar degree of oxidation. Sulfate contributes the second highest to NR-PM₁. Sulfate concentration is higher in summer (3.0 to 4.0 $\mu\text{g m}^{-3}$) than winter (1.4 to 1.7 $\mu\text{g m}^{-3}$), probably due to stronger photochemistry in summer. In contrast to sulfate, inorganic nitrate concentration is estimated to be tripled in winter than summer. This is likely caused by higher NO_x levels in winter, which serves as the source for inorganic nitrates and the semi-volatile nature of inorganic nitrates, which tend to partition into the particle phase when the temperature is low.

Positive Matrix Factorization (PMF) analysis revealed that the organic aerosol has various sources in the southeastern US, which changes between seasons and sampling sites (rural vs. urban). Hydrocarbon-like organic aerosol (HOA) and cooking organic aerosol (COA), which arise from primary vehicle emissions and cooking, respectively, are important but not dominant OA sources for urban sites. Biomass burning OA (BBOA) concentrations shows clear enhancements in winter compared to summer. In addition, biomass burning is found to be an important, but not exclusive, source for brown carbon in the southeastern US. Isoprene-derived OA (Isoprene-OA), which is from the reactive uptake of isoprene epoxides in the presence of hydrated sulfate, only exists in warmer months (May–August) when the isoprene emission is substantial. In addition to rural sites, Isoprene-OA is resolved from urban sites where the majority of peroxy radicals are believed to react with NO_x. We note that $f_{\text{C}_5\text{H}_6\text{O}^+}$, which has been used as a marker for Isoprene-OA, ranges from 0.9–2.3% and is higher in the Isoprene-

Aerosol characterization over the southeastern United States

L. Xu et al.

Title Page

Abstract

Introduction

Conclusions

References

Tables

Figures



Back

Close

Full Screen / Esc

Printer-friendly Version

Interactive Discussion



**Aerosol
characterization over
the southeastern
United States**

L. Xu et al.

Title Page

Abstract

Introduction

Conclusions

References

Tables

Figures



Back

Close

Full Screen / Esc

Printer-friendly Version

Interactive Discussion



Allan, J. D., Bower, K. N., Coe, H., Boudries, H., Jayne, J. T., Canagaratna, M. R., Millet, D. B., Goldstein, A. H., Quinn, P. K., Weber, R. J., and Worsnop, D. R.: Submicron aerosol composition at Trinidad Head, California, during ITCT 2K2: its relationship with gas phase volatile organic carbon and assessment of instrument performance, *J. Geophys. Res.-Atmos.*, 109, D23S24, doi:10.1029/2003JD004208, 2004.

Allan, J. D., Williams, P. I., Morgan, W. T., Martin, C. L., Flynn, M. J., Lee, J., Nemitz, E., Phillips, G. J., Gallagher, M. W., and Coe, H.: Contributions from transport, solid fuel burning and cooking to primary organic aerosols in two UK cities, *Atmos. Chem. Phys.*, 10, 647–668, doi:10.5194/acp-10-647-2010, 2010.

Andreae, M. O. and Gelencsér, A.: Black carbon or brown carbon? The nature of light-absorbing carbonaceous aerosols, *Atmos. Chem. Phys.*, 6, 3131–3148, doi:10.5194/acp-6-3131-2006, 2006.

Bae, M. S., Schwab, J. J., Zhang, Q., Hogrefe, O., Demerjian, K. L., Weimer, S., Rhoads, K., Orsini, D., Venkatchari, P., and Hopke, P. K.: Interference of organic signals in highly time resolved nitrate measurements by low mass resolution aerosol mass spectrometry, *J. Geophys. Res.-Atmos.*, 112, D22305, doi:10.1029/2007jd008614, 2007.

Bahreini, R., Ervens, B., Middlebrook, A. M., Warneke, C., de Gouw, J. A., DeCarlo, P. F., Jimenez, J. L., Brock, C. A., Neuman, J. A., Ryerson, T. B., Stark, H., Atlas, E., Brioude, J., Fried, A., Holloway, J. S., Peischl, J., Richter, D., Walega, J., Weibring, P., Wollny, A. G., and Fehsenfeld, F. C.: Organic aerosol formation in urban and industrial plumes near Houston and Dallas, Texas, *J. Geophys. Res.-Atmos.*, 114, D00F16, doi:10.1029/2008JD011493, 2009.

Blanchard, C. L., Hidy, G. M., Tanenbaum, S., Edgerton, E., Hartsell, B., and Jansen, J.: Carbon in southeastern US aerosol particles: empirical estimates of secondary organic aerosol formation, *Atmos. Environ.*, 42, 6710–6720, doi:10.1016/j.atmosenv.2008.04.011, 2008.

Blanchard, C. L., Hidy, G. M., Tanenbaum, S., and Edgerton, E. S.: NMOC, ozone, and organic aerosol in the southeastern United States, 1999–2007: 3. Origins of organic aerosol in Atlanta, Georgia, and surrounding areas, *Atmos. Environ.*, 45, 1291–1302, doi:10.1016/j.atmosenv.2010.12.004, 2011.

Blanchard, C. L., Hidy, G. M., Tanenbaum, S., Edgerton, E. S., and Hartsell, B. E.: The Southeastern Aerosol Research and Characterization (SEARCH) study: spatial variations and chemical climatology, 1999–2010, *J. Air Waste Manage.*, 63, 260–275, doi:10.1080/10962247.2012.749816, 2013.

**Aerosol
characterization over
the southeastern
United States**

L. Xu et al.

Title Page

Abstract

Introduction

Conclusions

References

Tables

Figures



Back

Close

Full Screen / Esc

Printer-friendly Version

Interactive Discussion



Bougiatioti, A., Stavroulas, I., Kostenidou, E., Zarrmpas, P., Theodosi, C., Kouvarakis, G., Canonaco, F., Prévôt, A. S. H., Nenes, A., Pandis, S. N., and Mihalopoulos, N.: Processing of biomass-burning aerosol in the eastern Mediterranean during summertime, *Atmos. Chem. Phys.*, 14, 4793–4807, doi:10.5194/acp-14-4793-2014, 2014.

5 Boyd, C. M., Sanchez, J., Xu, L., Eugene, A. J., Nah, T., Tuet, W. Y., Guzman, M. I., and Ng, N. L.: Secondary Organic Aerosol (SOA) formation from the β -pinene +NO₃ system: effect of humidity and peroxy radical fate, *Atmos. Chem. Phys. Discuss.*, 15, 2679–2744, doi:10.5194/acpd-15-2679-2015, 2015.

10 Bruns, E. A., Perraud, V., Zelenyuk, A., Ezell, M. J., Johnson, S. N., Yu, Y., Imre, D., Finlayson-Pitts, B. J., and Alexander, M. L.: Comparison of FTIR and particle mass spectrometry for the measurement of particulate organic nitrates, *Environ. Sci. Technol.*, 44, 1056–1061, doi:10.1021/es9029864, 2010.

15 Budisulistiorini, S. H., Canagaratna, M. R., Croteau, P. L., Marth, W. J., Baumann, K., Edgerton, E. S., Shaw, S. L., Knipping, E. M., Worsnop, D. R., Jayne, J. T., Gold, A., and Surratt, J. D.: Real-time continuous characterization of secondary organic aerosol derived from isoprene epoxydiols in Downtown Atlanta, Georgia, using the aerodyne aerosol chemical speciation monitor, *Environ. Sci. Technol.*, 47, 5686–5694, doi:10.1021/es400023n, 2013.

20 Canagaratna, M. R., Jayne, J. T., Jimenez, J. L., Allan, J. D., Alfarra, M. R., Zhang, Q., Onasch, T. B., Drewnick, F., Coe, H., Middlebrook, A., Delia, A., Williams, L. R., Trimborn, A. M., Northway, M. J., DeCarlo, P. F., Kolb, C. E., Davidovits, P., and Worsnop, D. R.: Chemical and microphysical characterization of ambient aerosols with the aerodyne aerosol mass spectrometer, *Mass Spectrom. Rev.*, 26, 185–222, 2007.

25 Canagaratna, M. R., Jimenez, J. L., Kroll, J. H., Chen, Q., Kessler, S. H., Massoli, P., Hildebrandt Ruiz, L., Fortner, E., Williams, L. R., Wilson, K. R., Surratt, J. D., Donahue, N. M., Jayne, J. T., and Worsnop, D. R.: Elemental ratio measurements of organic compounds using aerosol mass spectrometry: characterization, improved calibration, and implications, *Atmos. Chem. Phys.*, 15, 253–272, doi:10.5194/acp-15-253-2015, 2015.

30 Chen, Q., Farmer, D. K., Rizzo, L. V., Pauliquevis, T., Kuwata, M., Karl, T. G., Guenther, A., Allan, J. D., Coe, H., Andreae, M. O., Pöschl, U., Jimenez, J. L., Artaxo, P., and Martin, S. T.: Fine-mode organic mass concentrations and sources in the Amazonian wet season (AMAZE-08), *Atmos. Chem. Phys. Discuss.*, 14, 16151–16186, doi:10.5194/acpd-14-16151-2014, 2014.

**Aerosol
characterization over
the southeastern
United States**

L. Xu et al.

Title Page

Abstract

Introduction

Conclusions

References

Tables

Figures



Back

Close

Full Screen / Esc

Printer-friendly Version

Interactive Discussion



Cohan, D., Boylan, J., Marmur, A., and Khan, M.: An integrated framework for multipollutant air quality management and its application in Georgia, *Environ. Manage.*, 40, 545–554, doi:10.1007/s00267-006-0228-4, 2007.

5 Crippa, M., DeCarlo, P. F., Slowik, J. G., Mohr, C., Heringa, M. F., Chirico, R., Poulain, L., Freutel, F., Sciare, J., Cozic, J., Di Marco, C. F., Elsassner, M., Nicolas, J. B., Marchand, N., Abidi, E., Wiedensohler, A., Drewnick, F., Schneider, J., Borrmann, S., Nemitz, E., Zimmermann, R., Jaffrezo, J.-L., Prévôt, A. S. H., and Baltensperger, U.: Wintertime aerosol chemical composition and source apportionment of the organic fraction in the metropolitan area of Paris, *Atmos. Chem. Phys.*, 13, 961–981, doi:10.5194/acp-13-961-2013, 2013.

10 Crippa, M., Canonaco, F., Lanz, V. A., Äijälä, M., Allan, J. D., Carbone, S., Capes, G., Ceburnis, D., Dall'Osto, M., Day, D. A., DeCarlo, P. F., Ehn, M., Eriksson, A., Freney, E., Hildebrandt Ruiz, L., Hillamo, R., Jimenez, J. L., Junninen, H., Kiendler-Scharr, A., Kortelainen, A.-M., Kulmala, M., Laaksonen, A., Mensah, A. A., Mohr, C., Nemitz, E., O'Dowd, C., Ovadnevaite, J., Pandis, S. N., Petäjä, T., Poulain, L., Saarikoski, S., Sellegri, K., Swietlicki, E., Tiitta, P., Worsnop, D. R., Baltensperger, U., and Prévôt, A. S. H.: Organic aerosol components derived from 25 AMS data sets across Europe using a consistent ME-2 based source apportionment approach, *Atmos. Chem. Phys.*, 14, 6159–6176, doi:10.5194/acp-14-6159-2014, 2014.

20 Cubison, M. J., Ortega, A. M., Hayes, P. L., Farmer, D. K., Day, D., Lechner, M. J., Brune, W. H., Apel, E., Diskin, G. S., Fisher, J. A., Fuelberg, H. E., Hecobian, A., Knapp, D. J., Mikoviny, T., Riemer, D., Sachse, G. W., Sessions, W., Weber, R. J., Weinheimer, A. J., Wisthaler, A., and Jimenez, J. L.: Effects of aging on organic aerosol from open biomass burning smoke in aircraft and laboratory studies, *Atmos. Chem. Phys.*, 11, 12049–12064, doi:10.5194/acp-11-12049-2011, 2011.

25 Day, D. A., Wooldridge, P. J., Dillon, M. B., Thornton, J. A., and Cohen, R. C.: A thermal dissociation laser-induced fluorescence instrument for in situ detection of NO₂, peroxy nitrates, alkyl nitrates, and HNO₃, *J. Geophys. Res.-Atmos.*, 107, ACH 4-1–ACH 4-14, doi:10.1029/2001JD000779, 2002.

30 DeCarlo, P. F., Kimmel, J. R., Trimborn, A., Northway, M. J., Jayne, J. T., Aiken, A. C., Gonin, M., Fuhrer, K., Horvath, T., Docherty, K. S., Worsnop, D. R., and Jimenez, J. L.: Field-deployable, high-resolution, time-of-flight aerosol mass spectrometer, *Anal. Chem.*, 78, 8281–8289, doi:10.1021/ac061249n, 2006.

**Aerosol
characterization over
the southeastern
United States**

L. Xu et al.

Title Page

Abstract

Introduction

Conclusions

References

Tables

Figures



Back

Close

Full Screen / Esc

Printer-friendly Version

Interactive Discussion



- DeWitt, H. L., Hellebust, S., Temime-Roussel, B., Ravier, S., Polo, L., Jacob, V., Buisson, C., Charron, A., André, M., Pasquier, A., Besombes, J. L., Jaffrezo, J. L., Wortham, H., and Marchand, N.: Direct measurements of near-highway emissions in a high diesel environment, *Atmos. Chem. Phys. Discuss.*, 14, 27373–27424, doi:10.5194/acpd-14-27373-2014, 2014.
- 5 Eddingsaas, N. C., VanderVelde, D. G., and Wennberg, P. O.: Kinetics and products of the acid-catalyzed ring-opening of atmospherically relevant butyl epoxy alcohols, *J. Phys. Chem. A*, 114, 8106–8113, doi:10.1021/Jp103907c, 2010.
- Edgerton, E. S., Hartsell, B. E., Saylor, R. D., Jansen, J. J., Hansen, D. A., and Hidy, G. M.: The southeastern aerosol research and characterization study: Part II. Filter-based measure-
10 ments of fine and coarse particulate matter mass and composition, *J. Air Waste Manage.*, 55, 1527–1542, 2005.
- Ehn, M., Thornton, J. A., Kleist, E., Sipila, M., Junninen, H., Pullinen, I., Springer, M., Rubach, F., Tillmann, R., Lee, B., Lopez-Hilfiker, F., Andres, S., Acir, I.-H., Rissanen, M., Jokinen, T., Schobesberger, S., Kangasluoma, J., Kontkanen, J., Nieminen, T., Kurten, T.,
15 Nielsen, L. B., Jorgensen, S., Kjaergaard, H. G., Canagaratna, M., Maso, M. D., Berndt, T., Petaja, T., Wahner, A., Kerminen, V.-M., Kulmala, M., Worsnop, D. R., Wildt, J., and Mentel, T. F.: A large source of low-volatility secondary organic aerosol, *Nature*, 506, 476–479, doi:10.1038/nature13032, 2014.
- El Haddad, I., D’Anna, B., Temime-Roussel, B., Nicolas, M., Boreave, A., Favez, O., Voisin, D., Sciare, J., George, C., Jaffrezo, J.-L., Wortham, H., and Marchand, N.: Towards a better understanding of the origins, chemical composition and aging of oxygenated organic aerosols: case study of a Mediterranean industrialized environment, Marseille, *Atmos. Chem. Phys.*,
20 13, 7875–7894, doi:10.5194/acp-13-7875-2013, 2013.
- Farmer, D. K., Matsunaga, A., Docherty, K. S., Surratt, J. D., Seinfeld, J. H., Ziemann, P. J., and Jimenez, J. L.: Response of an aerosol mass spectrometer to organonitrates and organosulfates and implications for atmospheric chemistry, *P. Natl. Acad. Sci. USA*, 107, 6670–6675, doi:10.1073/pnas.0912340107, 2010.
- 25 Feng, Y., Ramanathan, V., and Kotamarthi, V. R.: Brown carbon: a significant atmospheric absorber of solar radiation?, *Atmos. Chem. Phys.*, 13, 8607–8621, doi:10.5194/acp-13-8607-2013, 2013.
- Ford, B. and Heald, C. L.: Aerosol loading in the Southeastern United States: reconciling surface and satellite observations, *Atmos. Chem. Phys.*, 13, 9269–9283, doi:10.5194/acp-13-9269-2013, 2013.

**Aerosol
characterization over
the southeastern
United States**

L. Xu et al.

Title Page

Abstract

Introduction

Conclusions

References

Tables

Figures



Back

Close

Full Screen / Esc

Printer-friendly Version

Interactive Discussion



sition and particulate organic nitrate formation in a boreal forestland–urban mixed region, *Atmos. Chem. Phys.*, 14, 13483–13495, doi:10.5194/acp-14-13483-2014, 2014.

Hayes, P. L., Ortega, A. M., Cubison, M. J., Froyd, K. D., Zhao, Y., Cliff, S. S., Hu, W. W., Toohey, D. W., Flynn, J. H., Lefer, B. L., Grossberg, N., Alvarez, S., Rappenglueck, B., Taylor, J. W., Allan, J. D., Holloway, J. S., Gilman, J. B., Kuster, W. C., De Gouw, J. A., Massoli, P., Zhang, X., Liu, J., Weber, R. J., Corrigan, A. L., Russell, L. M., Isaacman, G., Worton, D. R., Kreisberg, N. M., Goldstein, A. H., Thalman, R., Waxman, E. M., Volkamer, R., Lin, Y. H., Surratt, J. D., Kleindienst, T. E., Offenberg, J. H., Dusanter, S., Griffith, S., Stevens, P. S., Brioude, J., Angevine, W. M., and Jimenez, J. L.: Organic aerosol composition and sources in Pasadena, California, during the 2010 CalNex campaign, *J. Geophys. Res.-Atmos.*, 118, 9233–9257, doi:10.1002/Jgrd.50530, 2013.

Hecobian, A., Zhang, X., Zheng, M., Frank, N., Edgerton, E. S., and Weber, R. J.: Water-Soluble Organic Aerosol material and the light-absorption characteristics of aqueous extracts measured over the Southeastern United States, *Atmos. Chem. Phys.*, 10, 5965–5977, doi:10.5194/acp-10-5965-2010, 2010.

Hennigan, C. J., Sullivan, A. P., Fountoukis, C. I., Nenes, A., Hecobian, A., Vargas, O., Peltier, R. E., Case Hanks, A. T., Huey, L. G., Lefer, B. L., Russell, A. G., and Weber, R. J.: On the volatility and production mechanisms of newly formed nitrate and water soluble organic aerosol in Mexico City, *Atmos. Chem. Phys.*, 8, 3761–3768, doi:10.5194/acp-8-3761-2008, 2008.

Hennigan, C. J., Bergin, M. H., Russell, A. G., Nenes, A., and Weber, R. J.: Gas/particle partitioning of water-soluble organic aerosol in Atlanta, *Atmos. Chem. Phys.*, 9, 3613–3628, doi:10.5194/acp-9-3613-2009, 2009.

Hennigan, C. J., Miracolo, M. A., Engelhart, G. J., May, A. A., Presto, A. A., Lee, T., Sullivan, A. P., McMeeking, G. R., Coe, H., Wold, C. E., Hao, W.-M., Gilman, J. B., Kuster, W. C., de Gouw, J., Schichtel, B. A., Collett Jr., J. L., Kreidenweis, S. M., and Robinson, A. L.: Chemical and physical transformations of organic aerosol from the photo-oxidation of open biomass burning emissions in an environmental chamber, *Atmos. Chem. Phys.*, 11, 7669–7686, doi:10.5194/acp-11-7669-2011, 2011.

Hidy, G. M., Blanchard, C. L., Baumann, K., Edgerton, E., Tanenbaum, S., Shaw, S., Knipping, E., Tombach, I., Jansen, J., and Walters, J.: Chemical climatology of the southeastern United States, 1999–2013, *Atmos. Chem. Phys.*, 14, 11893–11914, doi:10.5194/acp-14-11893-2014, 2014.

**Aerosol
characterization over
the southeastern
United States**

L. Xu et al.

Title Page

Abstract

Introduction

Conclusions

References

Tables

Figures



Back

Close

Full Screen / Esc

Printer-friendly Version

Interactive Discussion



Hildebrandt, L., Engelhart, G. J., Mohr, C., Kostenidou, E., Lanz, V. A., Bougiatioti, A., DeCarlo, P. F., Prevot, A. S. H., Baltensperger, U., Mihalopoulos, N., Donahue, N. M., and Pandis, S. N.: Aged organic aerosol in the Eastern Mediterranean: the Finokalia Aerosol Measurement Experiment – 2008, *Atmos. Chem. Phys.*, 10, 4167–4186, doi:10.5194/acp-10-4167-2010, 2010.

Huang, X.-F., He, L.-Y., Hu, M., Canagaratna, M. R., Sun, Y., Zhang, Q., Zhu, T., Xue, L., Zeng, L.-W., Liu, X.-G., Zhang, Y.-H., Jayne, J. T., Ng, N. L., and Worsnop, D. R.: Highly time-resolved chemical characterization of atmospheric submicron particles during 2008 Beijing Olympic Games using an Aerodyne High-Resolution Aerosol Mass Spectrometer, *Atmos. Chem. Phys.*, 10, 8933–8945, doi:10.5194/acp-10-8933-2010, 2010.

Huffman, J. A., Docherty, K. S., Aiken, A. C., Cubison, M. J., Ulbrich, I. M., DeCarlo, P. F., Sueper, D., Jayne, J. T., Worsnop, D. R., Ziemann, P. J., and Jimenez, J. L.: Chemically-resolved aerosol volatility measurements from two megacity field studies, *Atmos. Chem. Phys.*, 9, 7161–7182, doi:10.5194/acp-9-7161-2009, 2009.

Isaacman, G., Kreisberg, N. M., Yee, L. D., Worton, D. R., Chan, A. W. H., Moss, J. A., Her-
ing, S. V., and Goldstein, A. H.: Online derivatization for hourly measurements of gas- and
particle-phase semi-volatile oxygenated organic compounds by thermal desorption aerosol
gas chromatography (SV-TAG), *Atmos. Meas. Tech.*, 7, 4417–4429, doi:10.5194/amt-7-4417-
2014, 2014.

Jacobs, M. I., Burke, W. J., and Elrod, M. J.: Kinetics of the reactions of isoprene-derived
hydroxynitrates: gas phase epoxide formation and solution phase hydrolysis, *Atmos. Chem.
Phys.*, 14, 8933–8946, doi:10.5194/acp-14-8933-2014, 2014.

Janssen, R. H. H., Vilà-Guerau de Arellano, J., Jimenez, J. L., Ganzeveld, L. N., Robin-
son, N. H., Allan, J. D., Coe, H., and Pugh, T. A. M.: Influence of boundary layer dynam-
ics and isoprene chemistry on the organic aerosol budget in a tropical forest, *J. Geophys.
Res.-Atmos.*, 118, 9351–9366, doi:10.1002/jgrd.50672, 2013.

Jathar, S. H., Gordon, T. D., Hennigan, C. J., Pye, H. O. T., Pouliot, G., Adams, P. J., Don-
ahue, N. M., and Robinson, A. L.: Unspeciated organic emissions from combustion sources
and their influence on the secondary organic aerosol budget in the United States, *P. Natl.
Acad. Sci. USA*, 111, 10473–10478, doi:10.1073/pnas.1323740111, 2014.

Jayne, J. T., Leard, D. C., Zhang, X. F., Davidovits, P., Smith, K. A., Kolb, C. E.,
and Worsnop, D. R.: Development of an aerosol mass spectrometer for size

**Aerosol
characterization over
the southeastern
United States**

L. Xu et al.

Title Page

Abstract

Introduction

Conclusions

References

Tables

Figures



Back

Close

Full Screen / Esc

Printer-friendly Version

Interactive Discussion



Orsini, D. A., Ma, Y. L., Sullivan, A., Sierau, B., Baumann, K., and Weber, R. J.: Refinements to the particle-into-liquid sampler (PILS) for ground and airborne measurements of water soluble aerosol composition, *Atmos. Environ.*, 37, 1243–1259, doi:10.1016/S1352-2310(02)01015-4, 2003.

5 Paatero, P.: A weighted non-negative least squares algorithm for three-way “PARAFAC” factor analysis, *Chemometrics Intell. Lab. Syst.*, 38, 223–242, 1997.

Paatero, P. and Tapper, U.: Positive Matrix Factorization – a nonnegative factor model with optimal utilization of error-estimates of data values, *Environmetrics*, 5, 111–126, doi:10.1002/env.3170050203, 1994.

10 Paglione, M., Kiendler-Scharr, A., Mensah, A. A., Finessi, E., Giulianelli, L., Sandrini, S., Facchini, M. C., Fuzzi, S., Schlag, P., Piazzalunga, A., Tagliavini, E., Henzing, J. S., and Decesari, S.: Identification of humic-like substances (HULIS) in oxygenated organic aerosols using NMR and AMS factor analyses and liquid chromatographic techniques, *Atmos. Chem. Phys.*, 14, 25–45, doi:10.5194/acp-14-25-2014, 2014.

15 Paulot, F., Crounse, J. D., Kjaergaard, H. G., Kurten, A., St Clair, J. M., Seinfeld, J. H., and Wennberg, P. O.: Unexpected epoxide formation in the gas-phase photooxidation of isoprene, *Science*, 325, 730–733, doi:10.1126/science.1172910, 2009.

Perring, A. E., Pusede, S. E., and Cohen, R. C.: An observational perspective on the atmospheric impacts of alkyl and multifunctional nitrates on ozone and secondary organic aerosol, *Chem. Rev.*, 113, 5848–5870, doi:10.1021/Cr300520x, 2013.

20 Piletic, I. R., Edney, E. O., and Bartolotti, L. J.: A computational study of acid catalyzed aerosol reactions of atmospherically relevant epoxides, *Phys. Chem. Chem. Phys.*, 15, 18065–18076, doi:10.1039/C3CP52851K, 2013.

25 Platt, S. M., El Haddad, I., Zardini, A. A., Clairotte, M., Astorga, C., Wolf, R., Slowik, J. G., Temime-Roussel, B., Marchand, N., Ježek, I., Drinovec, L., Močnik, G., Möhler, O., Richter, R., Barmet, P., Bianchi, F., Baltensperger, U., and Prévôt, A. S. H.: Secondary organic aerosol formation from gasoline vehicle emissions in a new mobile environmental reaction chamber, *Atmos. Chem. Phys.*, 13, 9141–9158, doi:10.5194/acp-13-9141-2013, 2013.

30 Presto, A. A., Gordon, T. D., and Robinson, A. L.: Primary to secondary organic aerosol: evolution of organic emissions from mobile combustion sources, *Atmos. Chem. Phys.*, 14, 5015–5036, doi:10.5194/acp-14-5015-2014, 2014.

Raatikainen, T., Vaattovaara, P., Tiitta, P., Miettinen, P., Rautiainen, J., Ehn, M., Kulmala, M., Laaksonen, A., and Worsnop, D. R.: Physicochemical properties and origin of organic groups

**Aerosol
characterization over
the southeastern
United States**

L. Xu et al.

Title Page

Abstract

Introduction

Conclusions

References

Tables

Figures



Back

Close

Full Screen / Esc

Printer-friendly Version

Interactive Discussion



detected in boreal forest using an aerosol mass spectrometer, *Atmos. Chem. Phys.*, 10, 2063–2077, doi:10.5194/acp-10-2063-2010, 2010.

Robinson, A. L., Donahue, N. M., Shrivastava, M. K., Weitkamp, E. A., Sage, A. M., Grieshop, A. P., Lane, T. E., Pierce, J. R., and Pandis, S. N.: Rethinking organic aerosols: semivolatile emissions and photochemical aging, *Science*, 315, 1259–1262, 2007.

Robinson, N. H., Hamilton, J. F., Allan, J. D., Langford, B., Oram, D. E., Chen, Q., Docherty, K., Farmer, D. K., Jimenez, J. L., Ward, M. W., Hewitt, C. N., Barley, M. H., Jenkin, M. E., Rickard, A. R., Martin, S. T., McFiggans, G., and Coe, H.: Evidence for a significant proportion of Secondary Organic Aerosol from isoprene above a maritime tropical forest, *Atmos. Chem. Phys.*, 11, 1039–1050, doi:10.5194/acp-11-1039-2011, 2011a.

Robinson, N. H., Newton, H. M., Allan, J. D., Irwin, M., Hamilton, J. F., Flynn, M., Bower, K. N., Williams, P. I., Mills, G., Reeves, C. E., McFiggans, G., and Coe, H.: Source attribution of Bornean air masses by back trajectory analysis during the OP3 project, *Atmos. Chem. Phys.*, 11, 9605–9630, doi:10.5194/acp-11-9605-2011, 2011b.

Rollins, A. W., Fry, J. L., Hunter, J. F., Kroll, J. H., Worsnop, D. R., Singaram, S. W., and Cohen, R. C.: Elemental analysis of aerosol organic nitrates with electron ionization high-resolution mass spectrometry, *Atmos. Meas. Tech.*, 3, 301–310, doi:10.5194/amt-3-301-2010, 2010.

Rollins, A. W., Browne, E. C., Min, K.-E., Pusede, S. E., Wooldridge, P. J., Gentner, D. R., Goldstein, A. H., Liu, S., Day, D. A., Russell, L. M., and Cohen, R. C.: Evidence for NO_x control over nighttime SOA formation, *Science*, 337, 1210–1212, doi:10.1126/science.1221520, 2012.

Russell, A., Holmes, H., Friberg, M., Ivey, C., Hu, Y., Balachandran, S., Mulholland, J., Tolbert, P., Sarnat, J., Sarnat, S., Strickland, M., Chang, H., and Liu, Y.: Use of air quality modeling results in health effects research, in: *Air Pollution Modeling and its Application XXIII*, edited by: Steyn, D. and Mathur, R., Springer Proceedings in Complexity, Springer International Publishing, 1–5, 2014.

Sato, K., Takami, A., Ito, T., Hikida, T., Shimono, A., and Imamura, T.: Mass spectrometric study of secondary organic aerosol formed from the photo-oxidation of aromatic hydrocarbons, *Atmos. Environ.*, 44, 1080–1087, doi:10.1016/j.atmosenv.2009.12.013, 2010.

Schichtel, B. A., Malm, W. C., Bench, G., Fallon, S., McDade, C. E., Chow, J. C., and Watson, J. G.: Fossil and contemporary fine particulate carbon fractions at 12

**Aerosol
characterization over
the southeastern
United States**

L. Xu et al.

Title Page

Abstract

Introduction

Conclusions

References

Tables

Figures



Back

Close

Full Screen / Esc

Printer-friendly Version

Interactive Discussion



rural and urban sites in the United States, *J. Geophys. Res.-Atmos.*, 113, D02311, doi:10.1029/2007JD008605, 2008.

Schneider, J., Weimer, S., Drewnick, F., Borrmann, S., Helas, G., Gwaze, P., Schmid, O., Andreae, M. O., and Kirchner, U.: Mass spectrometric analysis and aerodynamic properties of various types of combustion-related aerosol particles, *Int. J. Mass Spectrom.*, 258, 37–49, doi:10.1016/j.ijms.2006.07.008, 2006.

Setyan, A., Zhang, Q., Merkel, M., Knighton, W. B., Sun, Y., Song, C., Shilling, J. E., Onasch, T. B., Herndon, S. C., Worsnop, D. R., Fast, J. D., Zaveri, R. A., Berg, L. K., Wiedensohler, A., Flowers, B. A., Dubey, M. K., and Subramanian, R.: Characterization of submicron particles influenced by mixed biogenic and anthropogenic emissions using high-resolution aerosol mass spectrometry: results from CARES, *Atmos. Chem. Phys.*, 12, 8131–8156, doi:10.5194/acp-12-8131-2012, 2012.

Slowik, J. G., Vlasenko, A., McGuire, M., Evans, G. J., and Abbatt, J. P. D.: Simultaneous factor analysis of organic particle and gas mass spectra: AMS and PTR-MS measurements at an urban site, *Atmos. Chem. Phys.*, 10, 1969–1988, doi:10.5194/acp-10-1969-2010, 2010.

Slowik, J. G., Brook, J., Chang, R. Y.-W., Evans, G. J., Hayden, K., Jeong, C.-H., Li, S.-M., Liggio, J., Liu, P. S. K., McGuire, M., Mihele, C., Sjostedt, S., Vlasenko, A., and Abbatt, J. P. D.: Photochemical processing of organic aerosol at nearby continental sites: contrast between urban plumes and regional aerosol, *Atmos. Chem. Phys.*, 11, 2991–3006, doi:10.5194/acp-11-2991-2011, 2011.

Sun, Y. L., Zhang, Q., Schwab, J. J., Chen, W.-N., Bae, M.-S., Hung, H.-M., Lin, Y.-C., Ng, N. L., Jayne, J., Massoli, P., Williams, L. R., and Demerjian, K. L.: Characterization of near-highway submicron aerosols in New York City with a high-resolution aerosol mass spectrometer, *Atmos. Chem. Phys.*, 12, 2215–2227, doi:10.5194/acp-12-2215-2012, 2012a.

Sun, Y. L., Zhang, Q., Schwab, J. J., Yang, T., Ng, N. L., and Demerjian, K. L.: Factor analysis of combined organic and inorganic aerosol mass spectra from high resolution aerosol mass spectrometer measurements, *Atmos. Chem. Phys.*, 12, 8537–8551, doi:10.5194/acp-12-8537-2012, 2012b.

Surratt, J. D., Lewandowski, M., Offenberg, J. H., Jaoui, M., Kleindienst, T. E., Edney, E. O., and Seinfeld, J. H.: Effect of acidity on secondary organic aerosol formation from isoprene, *Environ. Sci. Technol.*, 41, 5363–5369, doi:10.1021/Es0704176, 2007.

Tsigaridis, K., Daskalakis, N., Kanakidou, M., Adams, P. J., Artaxo, P., Bahadur, R., Balkanski, Y., Bauer, S. E., Bellouin, N., Benedetti, A., Bergman, T., Berntsen, T. K., Beukes, J. P.,

**Aerosol
characterization over
the southeastern
United States**

L. Xu et al.

Title Page

Abstract

Introduction

Conclusions

References

Tables

Figures



Back

Close

Full Screen / Esc

Printer-friendly Version

Interactive Discussion



Bian, H., Carslaw, K. S., Chin, M., Curci, G., Diehl, T., Easter, R. C., Ghan, S. J., Gong, S. L., Hodzic, A., Hoyle, C. R., Iversen, T., Jathar, S., Jimenez, J. L., Kaiser, J. W., Kirkevåg, A., Koch, D., Kokkola, H., Lee, Y. H., Lin, G., Liu, X., Luo, G., Ma, X., Mann, G. W., Mihalopoulos, N., Morcrette, J.-J., Müller, J.-F., Myhre, G., Myriokefalitakis, S., Ng, N. L., O'Donnell, D., Penner, J. E., Pozzoli, L., Pringle, K. J., Russell, L. M., Schulz, M., Sciare, J., Seland, Ø., Shindell, D. T., Sillman, S., Skeie, R. B., Spracklen, D., Stavrou, T., Steenrod, S. D., Takemura, T., Tiitta, P., Tilmes, S., Tost, H., van Noije, T., van Zyl, P. G., von Salzen, K., Yu, F., Wang, Z., Wang, Z., Zaveri, R. A., Zhang, H., Zhang, K., Zhang, Q., and Zhang, X.: The AeroCom evaluation and intercomparison of organic aerosol in global models, *Atmos. Chem. Phys.*, 14, 10845–10895, doi:10.5194/acp-14-10845-2014, 2014.

Ulbrich, I. M., Canagaratna, M. R., Zhang, Q., Worsnop, D. R., and Jimenez, J. L.: Interpretation of organic components from Positive Matrix Factorization of aerosol mass spectrometric data, *Atmos. Chem. Phys.*, 9, 2891–2918, doi:10.5194/acp-9-2891-2009, 2009.

Verma, V., Fang, T., Guo, H., King, L., Bates, J. T., Peltier, R. E., Edgerton, E., Russell, A. G., and Weber, R. J.: Reactive oxygen species associated with water-soluble PM_{2.5} in the southeastern United States: spatiotemporal trends and source apportionment, *Atmos. Chem. Phys.*, 14, 12915–12930, doi:10.5194/acp-14-12915-2014, 2014.

Virkkula, A., Mäkelä, T., Hillamo, R., Yli-Tuomi, T., Hirsikko, A., Hämeri, K., and Koponen, I. K.: A simple procedure for correcting loading effects of Aethalometer data, *J. Air Waste Manage.*, 57, 1214–1222, doi:10.3155/1047-3289.57.10.1214, 2007.

Washenfelder, R. A., Attwood, A. R., Brock, C. A., Guo, H., Xu, L., Weber, R. J., Ng, N. L., Allen, H. M., Ayres, B. R., Baumann, K., Cohen, R. C., Draper, D. C., Duffey, K. C., Edgerton, E., Fry, J. L., Hu, W. W., Jimenez, J. L., Palm, B. B., Romer, P., Stone, E. A., Wooldridge, P. J., and Brown, S. S.: Biomass burning dominates brown carbon absorption in the rural southeastern United States, *Geophys. Res. Lett.*, 2014, GL062444, doi:10.1002/2014GL062444, 2015.

Weber, R.: Short-term temporal variation in PM_{2.5} mass and chemical composition during the Atlanta Supersite Experiment, 1999, *J. Air Waste Manage.*, 53, 84–91, doi:10.1080/10473289.2003.10466123, 2003.

Weber, R., Orsini, D., Duan, Y., Baumann, K., Kiang, C. S., Chameides, W., Lee, Y. N., Brechtel, F., Klotz, P., Jongejan, P., ten Brink, H., Slanina, J., Boring, C. B., Genfa, Z., Dasgupta, P., Hering, S., Stolzenburg, M., Dutcher, D. D., Edgerton, E., Hartsell, B., Solomon, P., and Tanner, R.: Intercomparison of near real time monitors of PM_{2.5} nitrate and sulfate at the U.S.

Aerosol characterization over the southeastern United States

L. Xu et al.

[Title Page](#)
[Abstract](#)
[Introduction](#)
[Conclusions](#)
[References](#)
[Tables](#)
[Figures](#)
[Back](#)
[Close](#)
[Full Screen / Esc](#)
[Printer-friendly Version](#)
[Interactive Discussion](#)


Environmental Protection Agency Atlanta Supersite, *J. Geophys. Res.-Atmos.*, 108, 8421, doi:10.1029/2001JD001220, 2003.

Weber, R. J., Sullivan, A. P., Peltier, R. E., Russell, A., Yan, B., Zheng, M., de Gouw, J., Warneke, C., Brock, C., Holloway, J. S., Atlas, E. L., and Edgerton, E.: A study of secondary organic aerosol formation in the anthropogenic-influenced southeastern United States, *J. Geophys. Res.-Atmos.*, 112, D13302, doi:10.1029/2007jd008408, 2007.

Winquist, A., Kirrane, E., Klein, M., Strickland, M., Darrow, L. A., Sarnat, S. E., Gass, K., Mulholland, J., Russell, A., and Tolbert, P.: Joint effects of ambient air pollutants on Pediatric Asthma Emergency Department visits in Atlanta, 1998–2004, *Epidemiology*, 25, 666–673, doi:10.1097/ede.0000000000000146, 2014.

Xu, L., Kollman, M. S., Song, C., Shilling, J. E., and Ng, N. L.: Effects of NO_x on the volatility of secondary organic aerosol from isoprene photooxidation, *Environ. Sci. Technol.*, 48, 2253–2262, doi:10.1021/es404842g, 2014.

Xu, L., Guo, H., Boyd, C. M., Klein, M., Bougiatioti, A., Cerully, K. M., Hite, J. R., Isaacman-VanWertz, G., Kreisberg, N. M., Knote, C., Olson, K., Koss, A., Goldstein, A. H., Hering, S. V., de Gouw, J., Baumann, K., Lee, S.-H., Nenes, A., Weber, R. J., and Ng, N. L.: Effects of anthropogenic emissions on aerosol formation from isoprene and monoterpenes in the southeastern United States, *P. Natl. Acad. Sci. USA*, 112, 37–42, doi:10.1073/pnas.1417609112, 2015.

Zhang, Q., Alfara, M. R., Worsnop, D. R., Allan, J. D., Coe, H., Canagaratna, M. R., and Jimenez, J. L.: Deconvolution and quantification of hydrocarbon-like and oxygenated organic aerosols based on aerosol mass spectrometry, *Environ. Sci. Technol.*, 39, 4938–4952, doi:10.1021/es048568l, 2005.

Zhang, Q., Jimenez, J. L., Canagaratna, M. R., Ulbrich, I. M., Ng, N. L., Worsnop, D. R., and Sun, Y. L.: Understanding atmospheric organic aerosols via factor analysis of aerosol mass spectrometry: a review, *Anal. Bioanal. Chem.*, 401, 3045–3067, doi:10.1007/s00216-011-5355-y, 2011.

Zhang, X., Hecobian, A., Zheng, M., Frank, N. H., and Weber, R. J.: Biomass burning impact on PM_{2.5} over the southeastern US during 2007: integrating chemically speciated FRM filter measurements, MODIS fire counts and PMF analysis, *Atmos. Chem. Phys.*, 10, 6839–6853, doi:10.5194/acp-10-6839-2010, 2010.

Zhang, X., Liu, Z., Hecobian, A., Zheng, M., Frank, N. H., Edgerton, E. S., and Weber, R. J.: Spatial and seasonal variations of fine particle water-soluble organic carbon (WSOC) over

**Aerosol
characterization over
the southeastern
United States**

L. Xu et al.

Title Page

Abstract

Introduction

Conclusions

References

Tables

Figures

◀

▶

◀

▶

Back

Close

Full Screen / Esc

Printer-friendly Version

Interactive Discussion



the southeastern United States: implications for secondary organic aerosol formation, *Atmos. Chem. Phys.*, 12, 6593–6607, doi:10.5194/acp-12-6593-2012, 2012.

Zhao, R., Mungall, E. L., Lee, A. K. Y., Aljawhary, D., and Abbatt, J. P. D.: Aqueous-phase photooxidation of levoglucosan – a mechanistic study using aerosol time-of-flight chemical ionization mass spectrometry (Aerosol ToF-CIMS), *Atmos. Chem. Phys.*, 14, 9695–9706, doi:10.5194/acp-14-9695-2014, 2014.

Zheng, M., Cass, G. R., Schauer, J. J., and Edgerton, E. S.: Source apportionment of PM_{2.5} in the southeastern United States using solvent-extractable organic compounds as tracers, *Environ. Sci. Technol.*, 36, 2361–2371, doi:10.1021/es011275x, 2002.

Zheng, M., Ke, L., Edgerton, E. S., Schauer, J. J., Dong, M., and Russell, A. G.: Spatial distribution of carbonaceous aerosol in the southeastern United States using molecular markers and carbon isotope data, *J. Geophys. Res.-Atmos.*, 111, D10S06, doi:10.1029/2005JD006777, 2006.

Zotter, P., El-Haddad, I., Zhang, Y., Hayes, P. L., Zhang, X., Lin, Y.-H., Wacker, L., Schnelle-Kreis, J., Abbaszade, G., Zimmermann, R., Surratt, J. D., Weber, R., Jimenez, J. L., Szidat, S., Baltensperger, U., and Prévôt, A. S. H.: Diurnal cycle of fossil and nonfossil carbon using radiocarbon analyses during CalNex, *J. Geophys. Res.-Atmos.*, 119, 2013JD021114, doi:10.1002/2013JD021114, 2014.

Aerosol characterization over the southeastern United States

L. Xu et al.

Table 1. Sampling sites and periods for the SCAPE and SOAS studies. Meteorological conditions, mixing ratios of gas-phase species, and mass concentrations of black carbon and NR-PM₁ species for all datasets. Average \pm one standard deviation are reported.

AMS sampling site	Jefferson Street	Centreville	Yorkville	Georgia Tech	Jefferson Street	Yorkville	Roadside	
Sampling period	10 May 2012– 2 Jun 2012	1 Jun 2013– 15 Jul 2013	26 Jun 2012– 20 Jul 2012	20 Jul 2012– 4 Sep 2012	6 Nov 2012– 4 Dec 2012	5 Dec 2012– 10 Jan 2013	26 Jan 2013– 28 Feb 2013	
Abbreviation	JST_May	CTR_June	YRK_July	GT_Aug	JST_Nov	YRK_Dec	RS_Jan	
Met ^a	<i>T</i> (°C)	23.0 \pm 4.3	24.7 \pm 4.3	26.9 \pm 4.5	26.1 \pm 3.5	11.3 \pm 5.0	7.8 \pm 5.5	8.1 \pm 4.8
	RH (%)	65.8 \pm 19.3	82.9 \pm 15.3	61.9 \pm 18.5	71.2 \pm 17.2	64.5 \pm 20.6	74.2 \pm 20.1	64.6 \pm 25.3
	WS (m s ⁻¹)	1.6 \pm 1.1	1.9 \pm 0.9	2.3 \pm 1.1	1.3 \pm 0.8	1.3 \pm 0.9	3.4 \pm 1.7	2.1 \pm 1.4
Gas (ppb)	NO	4.1 \pm 13.0	0.1 \pm 0.2	0.1 \pm 0.1	N/A	32.1 \pm 60.2	0.3 \pm 0.8	N/A
	NO ₂	10.3 \pm 10.3	0.6 \pm 0.6	1.1 \pm 0.8	N/A	18.4 \pm 12.8	3.0 \pm 3.0	N/A
	SO ₂	0.4 \pm 0.7	0.3 \pm 0.7	0.4 \pm 0.5	N/A	1.2 \pm 1.7	0.6 \pm 1.1	N/A
	O ₃	39.0 \pm 21.9	26.4 \pm 12.4	41.1 \pm 17.0	N/A	18.8 \pm 14.5	28.8 \pm 8.3	N/A
PM _{2.5} (μg m ⁻³)	BC ^b	N/A	0.2 \pm 0.2	N/A	0.9 \pm 0.6	0.9 \pm 0.9	0.4 \pm 0.3	1.3 \pm 1.0
NR-PM ₁ (μg m ⁻³)	SO ₄	3.0 \pm 1.5	1.9 \pm 1.4	3.5 \pm 1.8	4.0 \pm 2.1	1.7 \pm 0.9	1.4 \pm 1.0	1.6 \pm 1.2
	NO ₃	0.4 \pm 0.3	0.1 \pm 0.1	0.3 \pm 0.2	0.4 \pm 0.4	1.2 \pm 1.1	0.8 \pm 0.8	1.4 \pm 1.3
	NH ₄	1.1 \pm 0.5	0.4 \pm 0.3	1.1 \pm 0.5	1.2 \pm 0.6	0.9 \pm 0.6	0.6 \pm 0.5	0.9 \pm 0.6
	Chl	0.03 \pm 0.03	0.01 \pm 0.01	0.03 \pm 0.03	0.02 \pm 0.01	0.06 \pm 0.07	0.04 \pm 0.07	0.06 \pm 0.11
	Org	9.1 \pm 4.3	5.0 \pm 4.0	11.2 \pm 6.4	9.6 \pm 4.4	7.9 \pm 5.1	3.2 \pm 2.3	4.7 \pm 3.6

^a Meteorological data at JST and YRK are recorded by Atmospheric Research & Analysis (ARA). Meteorological data at GT and RS are from JST during the same periods.

^b Black carbon concentration was measured by a seven-wavelength Aethalometer at GT_Aug and JST_Nov and by a multi-angle absorption photometer (MAAP) at CTR_June, YRK_Dec, and RS_Jan.

Title Page

Abstract

Introduction

Conclusions

References

Tables

Figures

◀

▶

◀

▶

Back

Close

Full Screen / Esc

Printer-friendly Version

Interactive Discussion



Aerosol characterization over the southeastern United States

L. Xu et al.

Table 2. A summary of organic nitrates estimation from NO_x^+ ratio method. R_{AN} represents the NO_x^+ ratio ($= \text{NO}^+ / \text{NO}_2^+$) for pure ammonium nitrate (AN). R_{meas} represents the NO_x^+ ratio from observation. $\text{NO}_{3,\text{meas}}$ represents the total nitrate functionality (from both organic and inorganic nitrates) as measured by the HR-ToF-AMS. $\text{NO}_{3,\text{org}}$ represents the nitrate functionality from organic nitrates, which is estimated from the NO_x^+ ratio method. ON and OA represent organic nitrate and organic aerosol, respectively.

Site	R_{AN}^{a}	R_{meas}	R with LO-OOA		$\text{NO}_{3,\text{org}}$ conc. ($\mu\text{g m}^{-3}$) ^d		$\text{NO}_{3,\text{org}}/\text{NO}_{3,\text{meas}}$		ON/OA ^e	
			$\text{NO}_{3,\text{meas}}$	$\text{NO}_{3,\text{org}}^{\text{b}}$	lower	upper	lower	upper	lower	upper
JST_May	1.73	4.47	0.68	0.78	0.19	0.27	0.55	0.68	0.07	0.14
CTR_June ^c	2.93	7.10	0.76	0.84	0.06	0.08	0.80	1.00	0.06	0.10
YRK_July	2.24	5.45	0.66	0.83	0.18	0.28	0.63	1.00	0.05	0.12
GT_Aug	2.26	6.17	0.56	0.70	0.21	0.33	0.64	0.99	0.07	0.16
JST_Nov	1.95	3.12	0.14	0.63	0.23	0.25	0.19	0.21	0.09	0.15
YRK_Dec	2.24	3.16	0.29	0.08	0.09	0.16	0.11	0.21	0.09	0.25
RS_Jan	2.62	2.78	0.46	-0.22	0.13	0.13	0.10	0.10	0.09	0.13

^a R_{AN} is determined from IE calibrations at each site.

^b The correlation (Pearson' R) between LO-OOA and $\text{NO}_{3,\text{org}}$ are obtained by using $R_{\text{ON}} = 10$ in the NO_x^+ ratio method.

^c For CTR_June, only 24 June–15 July data are reported in order to compare with results from AMS-IC method where a PM_{10} cyclone was used.

^d For CTR_June and YRK_July, the NO_x^+ ratio method with $R_{\text{ON}} = 10$ and PMF method define the lower and upper bound for $\text{NO}_{3,\text{org}}$, respectively; for JST_Nov, YRK_Dec, the PMF method and NO_x^+ ratio method with $R_{\text{ON}} = 10$ define the lower and upper bound, respectively; for RS_Jan, the PMF method defines both the lower and upper bound; for JST_May and GT_Aug, the NO_x^+ ratio method with $R_{\text{ON}} = 10$ and 5 defines the lower and upper bound, respectively.

^e The lower and upper bounds correspond to an assumed MW of organic nitrates of 200 and 300 g mol^{-1} .

Aerosol
characterization over
the southeastern
United States

L. Xu et al.

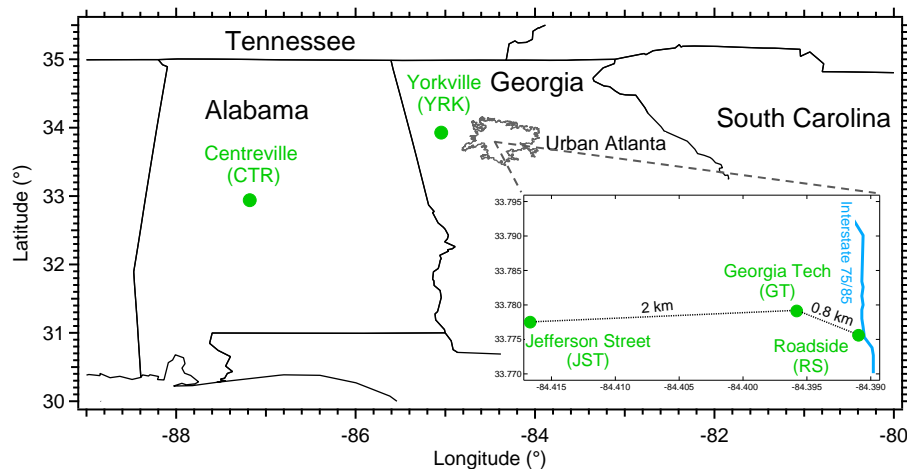


Figure 1. Sampling sites of SCAPE and SOAS studies. The gray circled region represents urban Atlanta.

[Title Page](#)[Abstract](#)[Introduction](#)[Conclusions](#)[References](#)[Tables](#)[Figures](#)[◀](#)[▶](#)[◀](#)[▶](#)[Back](#)[Close](#)[Full Screen / Esc](#)[Printer-friendly Version](#)[Interactive Discussion](#)

Aerosol characterization over the southeastern United States

L. Xu et al.

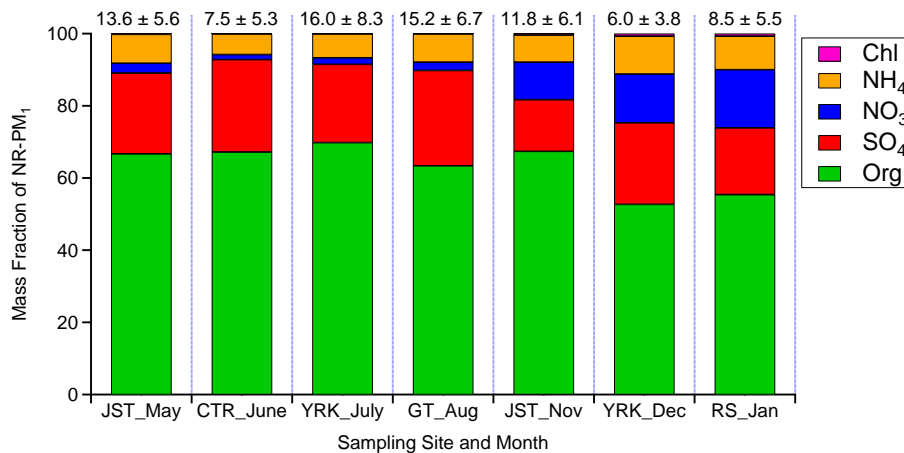


Figure 2. The mass fractions of non-refractory PM_1 (NR-PM_1) species measured by HR-ToF-AMS. The campaign average concentrations ($\mu\text{g m}^{-3}$) with one SD of total NR-PM_1 are listed at the top of the bar charts.

Title Page

Abstract

Introduction

Conclusions

References

Tables

Figures

◀

▶

◀

▶

Back

Close

Full Screen / Esc

Printer-friendly Version

Interactive Discussion



Aerosol characterization over the southeastern United States

L. Xu et al.

Title Page

Abstract

Introduction

Conclusions

References

Tables

Figures



Back

Close

Full Screen / Esc

Printer-friendly Version

Interactive Discussion

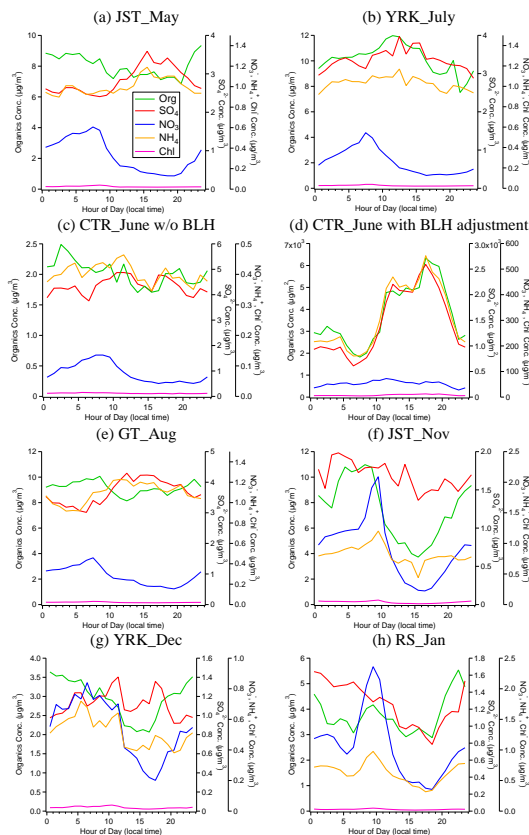


Figure 3. The diurnal profiles of non-refractory PM_1 (NR- PM_1) species measured by HR-ToF-AMS. Panel (d) shows the diurnal profiles of NR- PM_1 species after multiplying by the boundary layer height for the Centreville site.

Aerosol characterization over the southeastern United States

L. Xu et al.

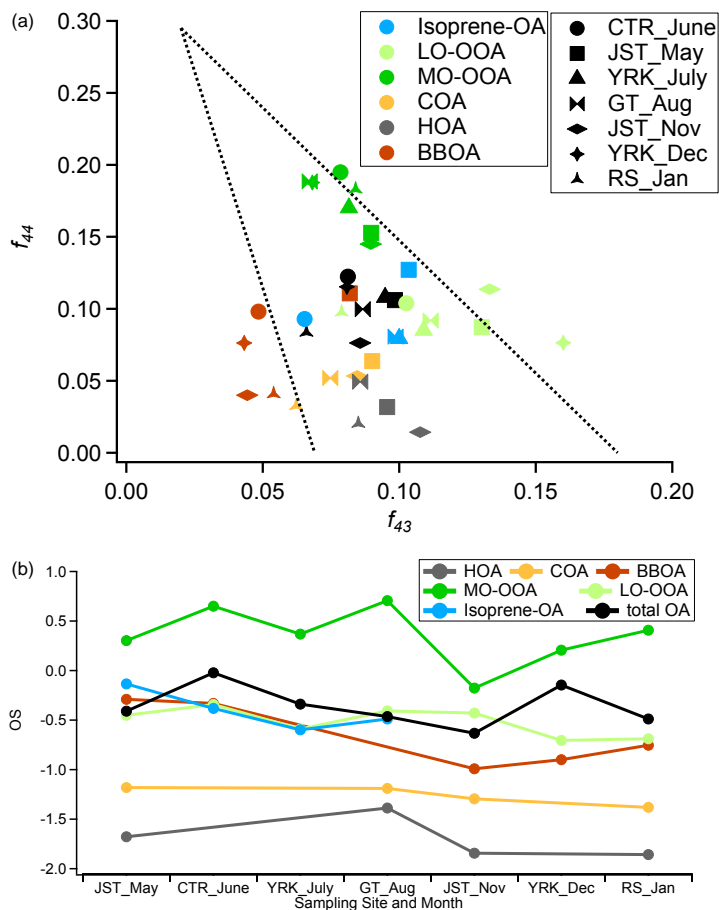


Figure 4. (a) f_{44} vs. f_{43} for total OA and OA factors resolved from PMF analysis. (b) The oxidation state of OA factors.

**Aerosol
characterization over
the southeastern
United States**

L. Xu et al.

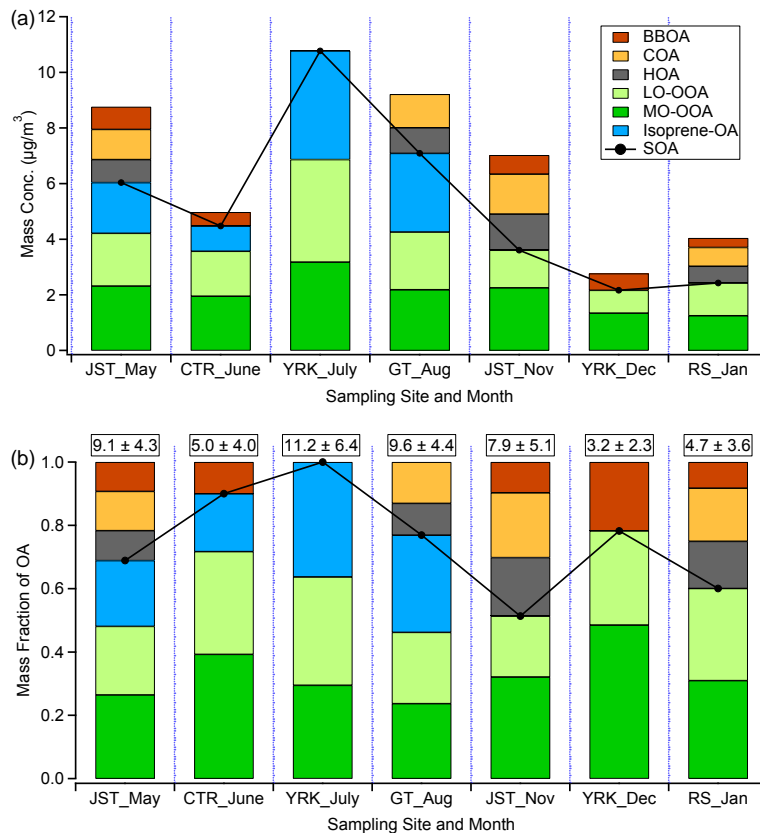


Figure 5. (a) The campaign average mass concentrations of OA factors resolved from PMF analysis. (b) The mass fractions of OA factors resolved from PMF analysis. The campaign average concentrations ($\mu\text{g m}^{-3}$) with one SD of total OA are listed at the top of the bar charts. SOA is the sum of Isoprene-OA, MO-OOA, and LO-OOA. POA is the sum of HOA, COA, and BBOA.

Title Page

Abstract Introduction

Conclusions References

Tables Figures

◀ ▶

◀ ▶

Back Close

Full Screen / Esc

Printer-friendly Version

Interactive Discussion



Aerosol characterization over the southeastern United States

L. Xu et al.

[Title Page](#)
[Abstract](#)
[Introduction](#)
[Conclusions](#)
[References](#)
[Tables](#)
[Figures](#)

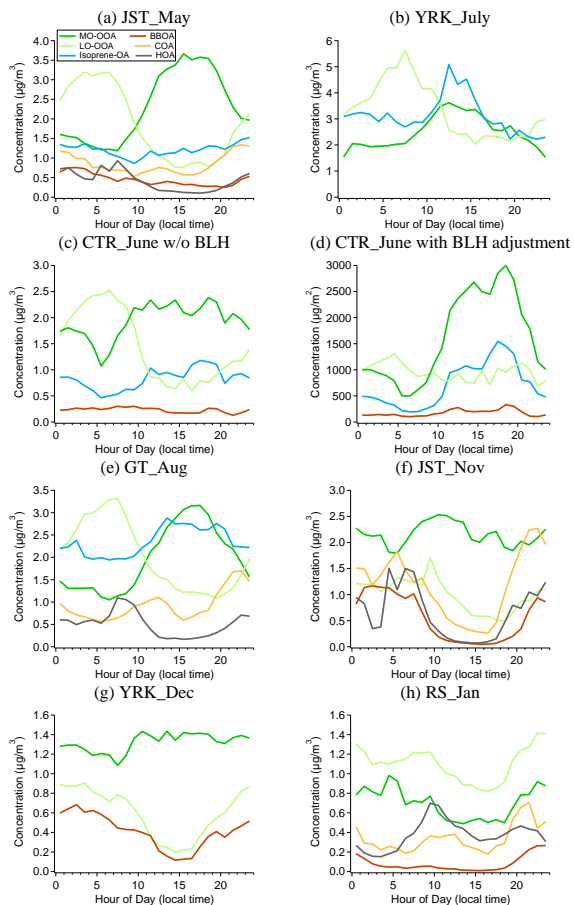
[Back](#)
[Close](#)
[Full Screen / Esc](#)
[Printer-friendly Version](#)
[Interactive Discussion](#)


Figure 6. The diurnal profiles of OA factors resolved from PMF analysis. **(d)** shows the diurnal profiles of OA factors after multiplying by the boundary layer height for the Centreville site.

Aerosol characterization over the southeastern United States

L. Xu et al.

Title Page

Abstract

Introduction

Conclusions

References

Tables

Figures



Back

Close

Full Screen / Esc

Printer-friendly Version

Interactive Discussion

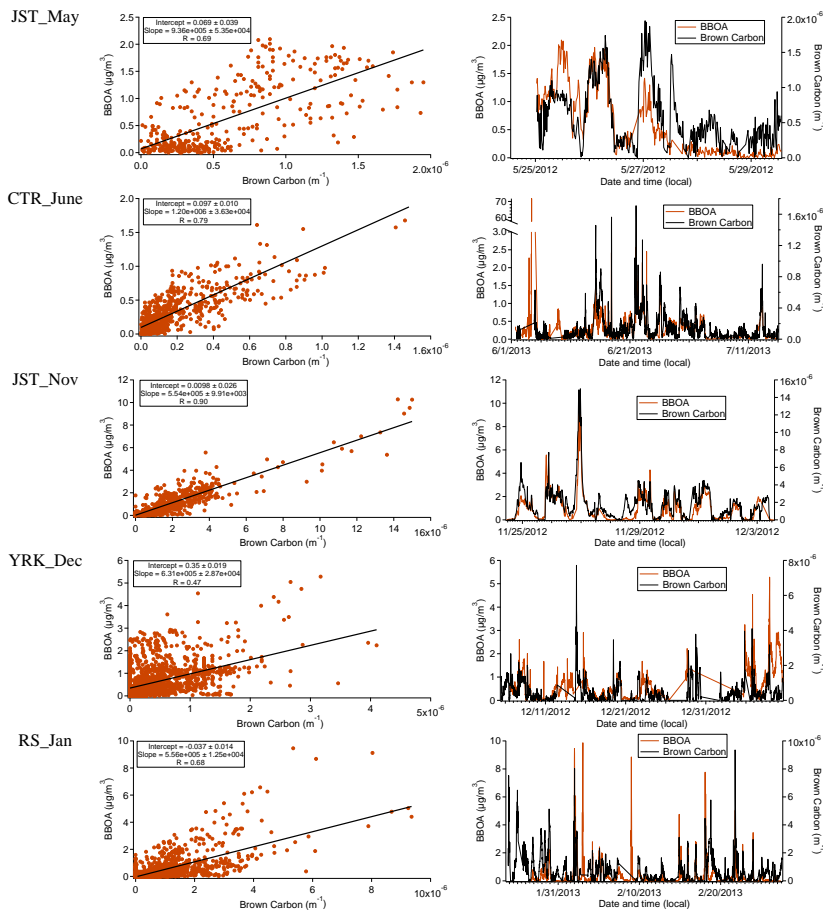


Figure 7. The scatter plot (left panel) and the time series (right panel) of BBOA and brown carbon for the datasets where BBOA factor is resolved.

Aerosol characterization over the southeastern United States

L. Xu et al.

Title Page

Abstract

Introduction

Conclusions

References

Tables

Figures



Back

Close

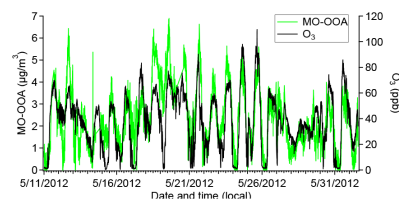
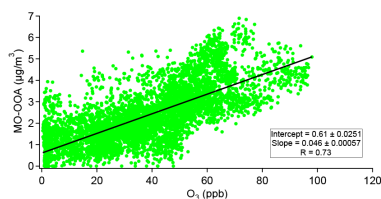
Full Screen / Esc

Printer-friendly Version

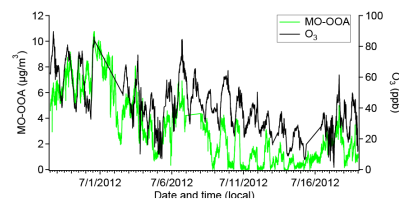
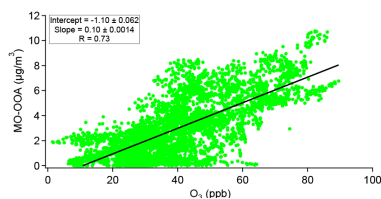
Interactive Discussion



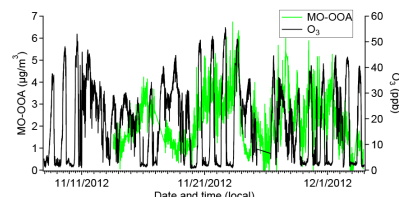
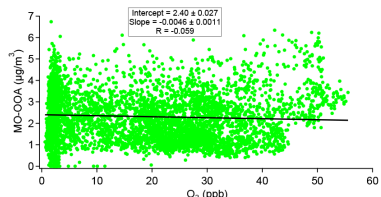
JST_May



YRK_July



JST_Nov



YRK_Dec

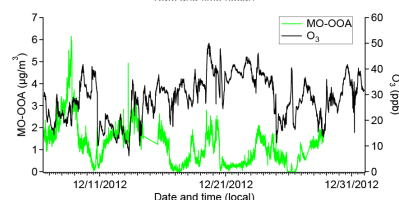
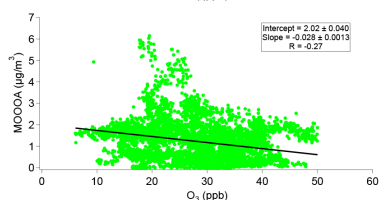


Figure 8. The scatter plot (left panel) and the time series (right panel) of MO-OOA and ozone.

Aerosol
 characterization over
 the southeastern
 United States

L. Xu et al.

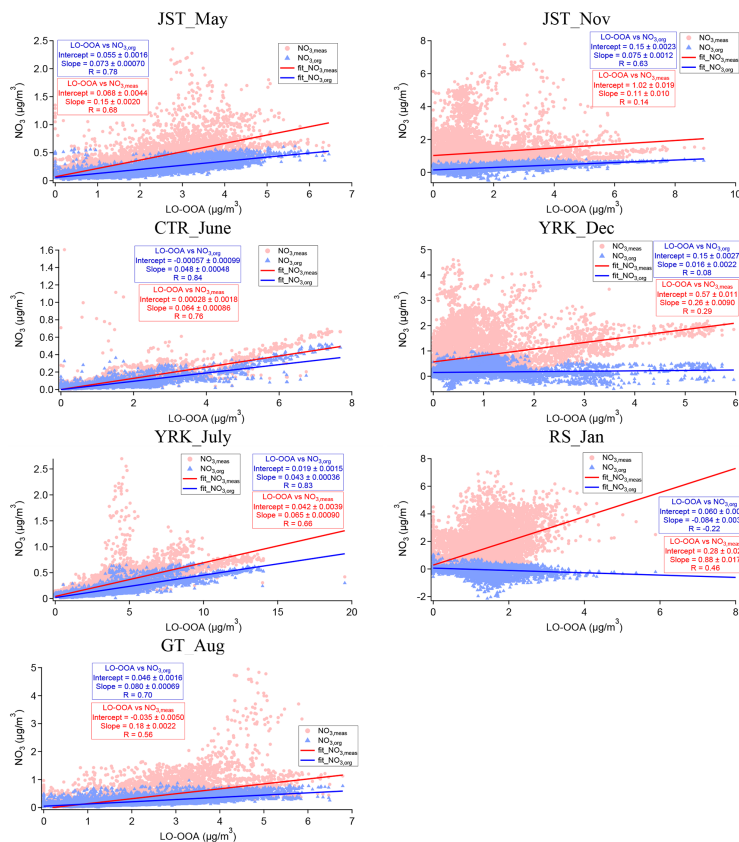


Figure 9. The scatter plot of LO-OOA vs. the total measured nitrates (i.e., NO_3, meas) and LO-OOA vs. estimated concentration of “nitrate functionality from organic nitrates” (i.e., NO_3, org) by using $R_{\text{ON}} = 10$ in the NO_x^+ ratio method.

Title Page

Abstract Introduction

Conclusions References

Tables Figures

◀ ▶

◀ ▶

Back Close

Full Screen / Esc

Printer-friendly Version

Interactive Discussion

Aerosol characterization over the southeastern United States

L. Xu et al.

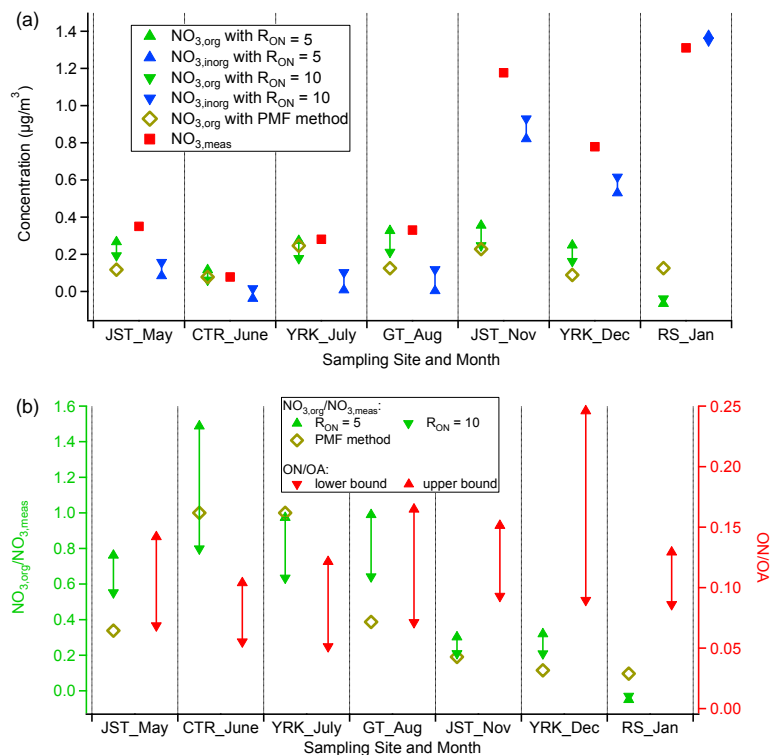


Figure 10. (a) The concentrations of total measured NO_3 (i.e., $\text{NO}_{3,\text{meas}}$), estimated “nitrate functional group from organic nitrates” (i.e., $\text{NO}_{3,\text{org}}$) by the NO_x^+ ratio method and the PMF method. (b) The contribution of $\text{NO}_{3,\text{org}}$ to $\text{NO}_{3,\text{meas}}$ (i.e., $\text{NO}_{3,\text{org}}/\text{NO}_{3,\text{meas}}$) from the NO_x^+ ratio method and the PMF method. Also shown are the estimated contribution of organic nitrates to total OA from the “best estimate” range of $\text{NO}_{3,\text{org}}$ and by assuming a MW of 200 and 300 g mol^{-1} of organic nitrates.

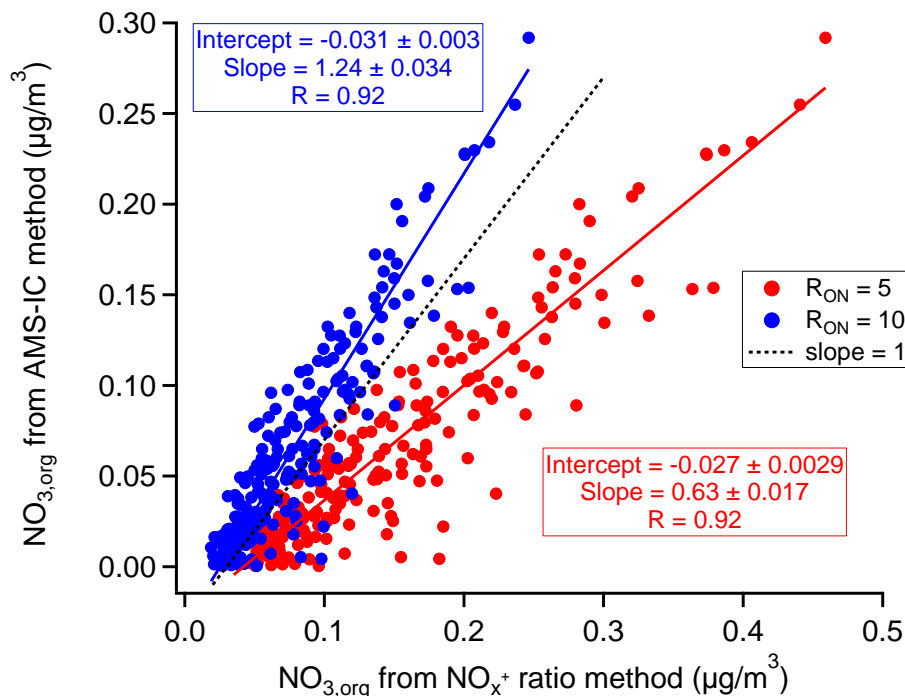


Figure 11. The comparison of estimated concentration of “nitrate functionality from organic nitrates” (i.e., $\text{NO}_{3,\text{org}}$) at Centreville site between the AMS-IC method and NO_x^+ ratio method with R_{ON} values of 5 and 10. The intercept and slope are obtained by orthogonal fit which considers the measurement errors in both dependent and independent variables. The correlation R is obtained by linear least-squares fit. The intercepts are within to the detection limit of PILS-IC nitrate (i.e., $0.03 \mu\text{g m}^{-3}$). The 1 : 1 line is offset by the detection limit of PILS-IC nitrate (i.e., $-0.03 \mu\text{g m}^{-3}$).

**Aerosol
characterization over
the southeastern
United States**

L. Xu et al.

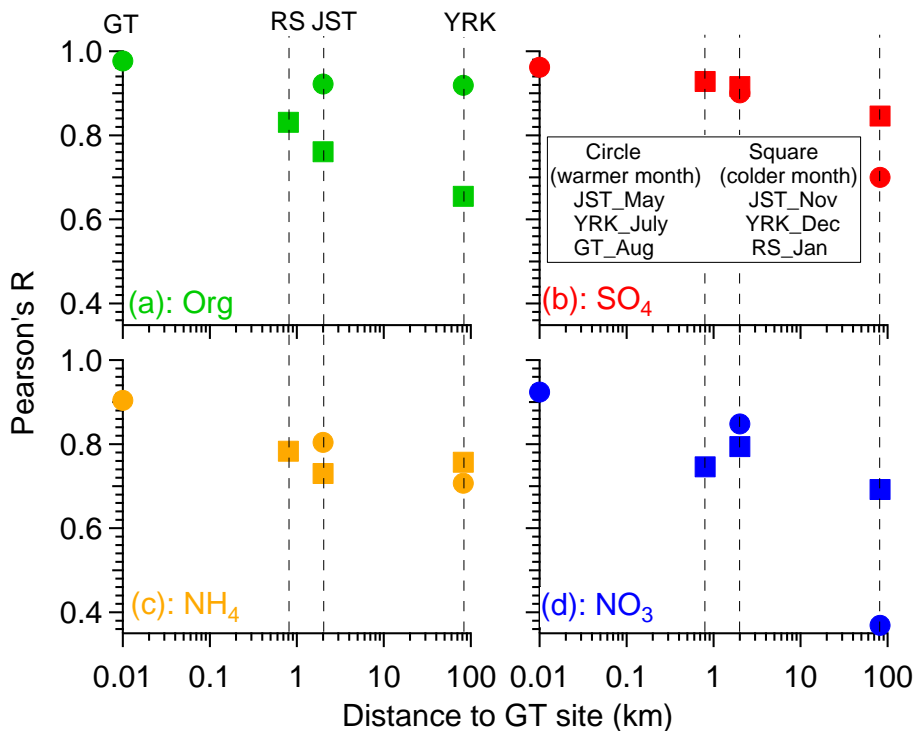


Figure 12. The correlations for NR-PM₁ species between ACSM measurements (stationary at the Georgia Tech site) and HR-ToF-AMS measurements (rotating among different sites). The dotted lines represent the sampling sites where the HR-ToF-AMS measurements were made.

Title Page

Abstract Introduction

Conclusions References

Tables Figures

◀ ▶

◀ ▶

Back Close

Full Screen / Esc

Printer-friendly Version

Interactive Discussion



Aerosol
characterization over
the southeastern
United States

L. Xu et al.

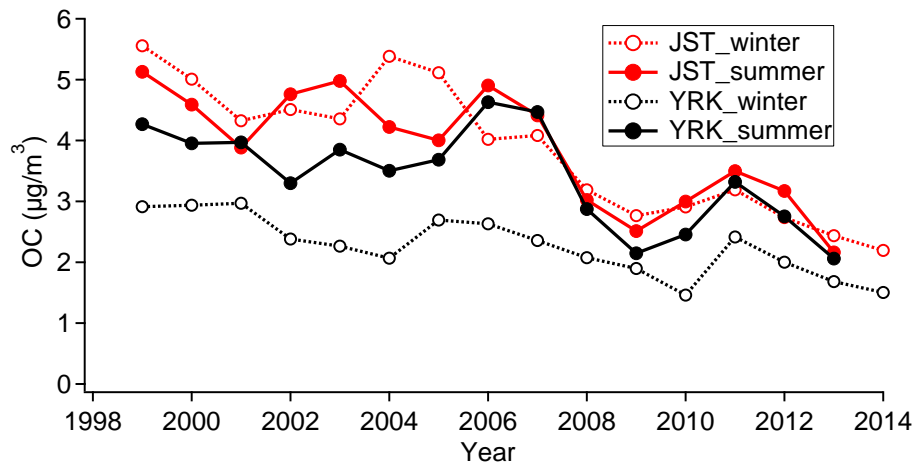


Figure 13. Mean seasonal concentrations of organic carbon at the Jefferson Street site and the Yorkville site. Summer: June–August. Winter: December–February.

Aerosol characterization over the southeastern United States

L. Xu et al.

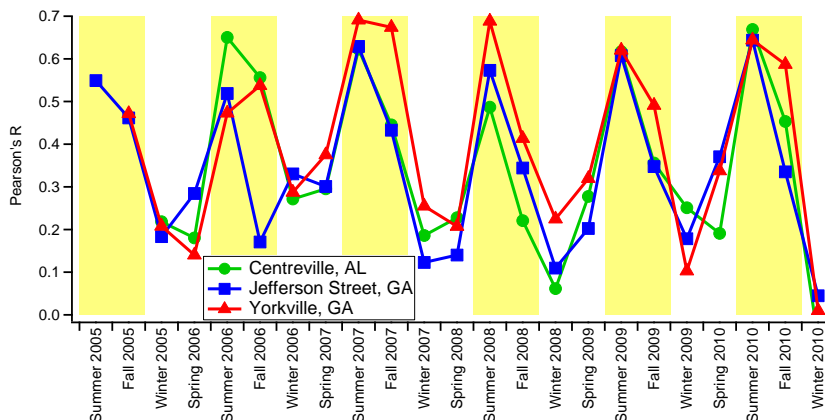


Figure 14. The seasonality of the correlation between organic carbon and sulfate at the Jefferson Street, Yorkville, and Centreville site. Seasons are by grouped by calendar months (Spring: March–May, Summer: June–August, Fall: September–November, and Winter: December–February).

Title Page

Abstract	Introduction
Conclusions	References
Tables	Figures

◀
▶

◀
▶

Back
Close

Full Screen / Esc

Printer-friendly Version

Interactive Discussion

